1521-0103/348/1/46–58$25.00
THE JOURNAL OF PHARMACOLOGY AND EXPERIMENTAL THERAPEUTICS

http://dx.doi.org/10.1124/jpet.113.208389
J Pharmacol Exp Ther 348:46–58, January 2014

The Unique $\alpha4(+)/(-)\alpha4$ Agonist Binding Site in $(\alpha4)_3(\beta2)_2$ Subtype Nicotinic Acetylcholine Receptors Permits Differential Agonist Desensitization Pharmacology versus the $(\alpha4)_2(\beta2)_3$ Subtype[S]

J. Brek Eaton, Linda M. Lucero, Harrison Stratton, Yongchang Chang, John F. Cooper, Jon M. Lindstrom, Ronald J. Lukas, and Paul Whiteaker

Division of Neurobiology, Barrow Neurologic Institute, Phoenix, Arizona (J.B.E., L.M.L., H.S., Y.C., R.J.L., P.W.); and Department of Neuroscience, Medical School of the University of Pennsylvania, Philadelphia, Pennsylvania (J.F.C., J.M.L.)

Received July 29, 2013; accepted November 1, 2013

ABSTRACT

Selected nicotinic agonists were used to activate and desensitize high-sensitivity (HS) $(\alpha4)_2(\beta2)_3$ or low-sensitivity (LS) $(\alpha4)_3(\beta2)_2$ isoforms of human $\alpha4\beta2$-nicotinic acetylcholine receptors (nAChRs). Function was assessed using $^{86}Rb^+$ efflux in a stably transfected SH-EP1-h$\alpha4\beta2$ human epithelial cell line, and two-electrode voltage-clamp electrophysiology in *Xenopus laevis* oocytes expressing concatenated pentameric HS or LS $\alpha4\beta2$-nAChR constructs (HSP and LSP). Unlike previously studied agonists, desensitization by the highly selective agonists A-85380 [3-(2(*S*)-azetidinylmethoxy)pyridine] and sazetidine-A (Saz-A) preferentially reduced $\alpha4\beta2$-nAChR HS-phase versus LS-phase responses. The concatenated-nAChR experiments confirmed that approximately 20% of LS-isoform acetylcholine-induced function occurs in an HS-like phase, which is abolished by Saz-A preincubation. Six mutant LSPs were generated, each targeting a conserved agonist binding residue within the LS-isoform-only $\alpha4(+)/(-)\alpha4$ interface agonist binding site. Every mutation reduced the percentage of LS-phase function, demonstrating that this site underpins LS-phase function. Oocyte-surface expression of the HSP and each of the LSP constructs was statistically indistinguishable, as measured using $\beta2$-subunit–specific [^{125}I]mAb295 labeling. However, maximum function is approximately five times greater on a "per-receptor" basis for unmodified LSP versus HSP $\alpha4\beta2$-nAChRs. Thus, recruitment of the $\alpha4(+)/(-)\alpha4$ site at higher agonist concentrations appears to augment otherwise-similar function mediated by the pair of $\alpha4(+)/(-)\beta2$ sites shared by both isoforms. These studies elucidate the receptor-level differences underlying the differential pharmacology of the two $\alpha4\beta2$-nAChR isoforms, and demonstrate that HS versus LS $\alpha4\beta2$-nAChR activity can be selectively manipulated using pharmacological approaches. Since $\alpha4\beta2$ nAChRs are the predominant neuronal subtype, these discoveries likely have significant functional implications, and may provide important insights for drug discovery and development.

Introduction

Nicotinic acetylcholine receptors (nAChRs) are prototypical members of the ligand-gated ion channel (LGIC) superfamily of neurotransmitter receptors. Vertebrate nAChRs exist as a diverse family of subtypes defined by their compositions as pentamers of homologous subunits derived from at least 17 genes ($\alpha1$–$\alpha10$, $\beta1$–$\beta4$, γ, δ, ε). Each nAChR subtype has characteristic pharmacological and biophysical properties that, nevertheless, can overlap with those of other subtypes (Gotti et al., 2009).

The predominant nAChR subtype in the brain, with high binding affinity for nicotine and other agonists, contains $\alpha4$ and $\beta2$ subunits ($\alpha4\beta2$-nAChR) (Whiting and Lindstrom, 1987; Flores et al., 1992). $\alpha4\beta2$-nAChRs have been implicated in perception, cognition, and emotion; in nicotine self-administration, reward, and dependence; as well as in diseases such as Alzheimer's and epilepsy (Picciotto et al., 1995; Cordero-Erausquin et al., 2000; Steinlein, 2001; Lindstrom, 2003). Initial evidence based on site-directed mutagenesis and immunochemical studies of heterologously expressed receptors indicated that $\alpha4\beta2$-nAChRs have an $(\alpha4)_2(\beta2)_3$ subunit stoichiometry (Anand et al., 1991; Cooper et al., 1991). However, later heterologous expression studies using *Xenopus laevis* oocytes showed that

This research was primarily supported by the National Institutes of Health National Institute on Drug Abuse [Grant R21-DA026627 (to P.W.)]. Additional funding was provided by the National Institutes of Health National Institute on Drug Abuse [Grant R01-DA012242 (to P.W.); R01-DA015389, R01-DA017980, U19-DA019375, and U19-DA019377 (to R.J.L.)]; the National Institutes of Health National Institute of Mental Health [Grant R01-MH085193 (to J.M.L)]; the National Institutes of Health National Institute of Neurological Disorders and Stroke [Grant R01-NS011323 (to J.M.L.)]; and the National Institutes of Health National Institute of General Medical Sciences [Grant R01-GM085237 (to Y.C.)]. The contents of this article do not necessarily reflect the views of the aforementioned awarding agencies.

J.B.E. and L.M.L. contributed equally to this work.

dx.doi.org/10.1124/jpet.113.208389.

[S] This article has supplemental material available at jpet.aspetjournals.org.

ABBREVIATIONS: A-85380, 3-(2(*S*)-azetidinylmethoxy)pyridine; ACh, acetylcholine; ANOVA, analysis of variance; CRC, concentration-response curve; HS, high sensitivity; HSP, high-sensitivity pentameric concatemer; LGIC, ligand-gated ion channel; LS, low sensitivity; LSP, low-sensitivity pentameric concatemer; nAChR, nicotinic acetylcholine receptor; NS9283, 3-[3-(pyridin-3-yl)-1,2,4-oxadiazol-5-yl]benzonitrile; OR2, oocyte Ringer's buffer; Saz-A, 6-(5-(((*S*)-azetidin-2-yl)methoxy)pyridine-3-yl)hex-5-yn-1-ol (also known as AMOP-H-OH).

when ratios of expressed nAChR $\alpha4$ and $\beta2$ subunits were manipulated, it was possible to produce two $\alpha4\beta2$-nAChR isoforms. When $\beta2$ subunit cRNA is present in approximately 10-fold excess over $\alpha4$ subunit cRNA, an isoform with high sensitivity (HS) to activation by agonists and a presumed $(\alpha4)_2(\beta2)_3$ stoichiometry is produced. In oocytes injected with the opposite subunit ratio (approximately 10:1 of $\alpha4$:$\beta2$ subunit cRNAs), an isoform with lower agonist sensitivity (LS) predominates, with a presumed $(\alpha4)_3(\beta2)_2$ stoichiometry (Zwart and Vijverberg, 1998). Related work in transfected cell lines reinforced the findings in oocytes (Nelson et al., 2003). Furthermore, agonist concentration-response curve (CRC) analyses in wild-type mice are consistent with the idea that a mixture of HS and LS $\alpha4\beta2$-nAChR isoforms is naturally expressed (Marks et al., 1999). Functional assessments in heterozygotic nAChR $\alpha4$- or $\beta2$-subunit–null mutant mice (which therefore express a biased ratio of these genes compared with wild-type mice) are consistent with of the concept that native HS and LS $\alpha4\beta2$-nAChR isoforms also have $\alpha4$:$\beta2$ subunit ratios of 2:3 and 3:2, respectively (Gotti et al., 2008). Work using linked-subunit (concatemeric) constructs allowed the expression of $\alpha4\beta2$-nAChRs with completely defined subunit compositions, and confirmed these putative stoichiometries (Zhou et al., 2003; Carbone et al., 2009). Recent studies show that $(\alpha4)_2(\beta2)_3$ and $(\alpha4)_3(\beta2)_2$ share the same pair of conserved, long-recognized, agonist binding sites present at the interfaces between the primary (+) face of the $\alpha4$ subunit and the complementary (−) face of the $\beta2$ subunit (i.e., at $\alpha4(+)/(-)\beta2$ interfaces). However, an additional binding site is located at the $\alpha4(+)/(-)\alpha4$ interface found only in LS $\alpha4\beta2$-nAChRs. Site-directed mutagenesis and covalent modification experiments demonstrate that the $\alpha4(+)/(-)\alpha4$ site is required for effective activation of $(\alpha4)_3(\beta2)_2$-nAChR, giving rise to their distinctive LS pharmacology (Harpsøe et al., 2011; Mazzaferro et al., 2011).

HS and LS $\alpha4\beta2$-nAChR isoforms have different sensitivities to the antagonists methyllycaconitine and dihydro-β-erythroidine (Marks et al., 1999), but concentrations at which agonists such as epibatidine, nicotine, cytisine, and methylcarbachol induce desensitization are not different between HS and LS $\alpha4\beta2$-nAChRs (Marks et al., 2010). However, none of these agonists is especially selective between activation of HS and LS nAChRs (Marks et al., 1999) or thus, presumably, between $\alpha4(+)/(-)\beta2$ and $\alpha4(+)/(-)\alpha4$ agonist binding sites. In this study, we sought to use more discriminating ligands to dissect the roles played by $\alpha4(+)/(-)\beta2$ and $\alpha4(+)/(-)\alpha4$ interfaces in HS and/or LS $\alpha4\beta2$-nAChR isoforms. We investigated activation and desensitization of receptors in response to acetylcholine (ACh) and to two highly HS- versus LS-selective nicotinic agonists that might better discriminate between $\alpha4\beta2$-nAChR isoforms: A-85380 [3-(2(*S*)-azetidinylmethoxy)pyridine] (Abreo et al., 1996) and sazetidine-A [6-(5-(((*S*)-azetidin-2-yl)methoxy)pyridine-3-yl)hex-5-yn-1-ol; henceforth abbreviated as Saz-A] (Xiao et al., 2006). We report that HS-phase $\alpha4\beta2$-nAChR responses can be selectively inactivated by low concentrations of either ligand, while leaving LS-phase responses in a state that can still be activated by acute agonist application. We also show that single residue mutations targeted to $\alpha4(+)/(-)\alpha4$ interfaces can affect functional activity, the balance of HS- versus LS-phase activation, and agonist sensitivity of $(\alpha4)_3(\beta2)_2$-nAChRs, further demonstrating the functional significance of this recently recognized site. These findings, especially when coupled with the realization that different $\alpha4\beta2$-nAChR isoforms will respond differently to endogenous concentrations of ACh and the presence of exogenous nicotinic agonists, suggest novel drug discovery and development opportunities for $\alpha4\beta2$-AChR. These possibilities may also apply to other members of the LGIC superfamily that also contain ligand-binding subunit interfaces related to the recently discovered $\alpha4/\alpha4$ site.

Materials and Methods

Chemicals other than those kindly provided by Drs. Alan Kozikowski (University of Illinois, Chicago, IL) or F. Ivy Carroll (Research Triangle Institute, Research Triangle Park, NC) were sourced from Sigma-Aldrich Co. LLC (St. Louis, MO) unless specified otherwise.

Cell Culture. Cells of the SH-EP1 human epithelial cell line were kindly provided by Dr. June Biedler (Sloan-Kettering Institute for Cancer Research, New York, NY). SH-EP1-h$\alpha4\beta2$ cells [stably transfected SH-EP1 epithelial cells heterologously expressing human $\alpha4\beta2$-nAChR (Eaton et al., 2003)] were grown in Dulbecco's modified Eagle's medium (high glucose, bicarbonate-buffered, with 1 mM sodium pyruvate and 8 mM L-glutamine) supplemented with 100 U/ml penicillin and 100 μg/ml streptomycin (all from MediaTech, Inc., Manassas, VA) plus 10% horse serum (Life Technologies, Inc., Gaithersburg, MD) and 5% fetal bovine serum (Atlanta Biologicals, Atlanta, GA) on 100-mm diameter tissue culture plates in a humidified atmosphere containing 5% CO_2 in air at 37°C (Eaton et al., 2003). Positive selection for expression of the $\alpha4$ and $\beta2$ subunits (in pcDNA3.1/Zeo and pcDNA3.1/Hygro, respectively; Invitrogen, Carlsbad, CA) was maintained by further supplementation of the growth medium with 0.25 mg/ml zeocin (Invitrogen) and 0.4 mg/ml hygromycin B (Calbiochem, San Diego, CA).

Cell Line nAChR Functional Assays ($^{86}Rb^+$ Efflux). Function of $\alpha4\beta2$-nAChRs expressed by human SH-EP1-h$\alpha4\beta2$ cells was determined using $^{86}Rb^+$ efflux assays (Lukas and Cullen, 1988). Cells were harvested at confluence from 100-mm plates by trypsinization (MediaTech, Inc.) before being resuspended in complete medium and evenly seeded at a density of 1.5 confluent 100-mm dishes per 24-well plate (BD Falcon, Franklin Lakes, NJ). After cells had adhered (generally overnight, but no sooner than 4 hours later), medium was removed and replaced with 250 μl per well of complete medium supplemented with approximately 300,000 cpm of $^{86}Rb^+$ (PerkinElmer Life and Analytical Sciences, Waltham, MA), counted at 40% efficiency using Cherenkov counting and a Packard TriCarb 1900 Liquid Scintillation Analyzer (PerkinElmer Life and Analytical Sciences). After $^{86}Rb^+$ loading for at least 4 hours (typically overnight), $^{86}Rb^+$ efflux was measured using the "flip-plate" technique (Gentry et al., 2003), first used to remove extracellular isotope by a rinse in efflux buffer (130 mM NaCl, 5.4 mM KCl, 2 mM $CaCl_2$, 5 mM glucose, 50 mM HEPES, pH 7.4; all at room temperature) followed by a 10-minute "preincubation" in a low, desensitizing concentration of agonist or in efflux buffer alone. Cells were then incubated for 5 minutes in the presence of ligands of choice at a range of concentrations in efflux buffer to define acute effects of drugs. Maximum efflux was defined in the presence of a maximally efficacious concentration of a full agonist (1 mM carbamylcholine; carbachol, which has been shown to be a full agonist in this assay) (Eaton et al., 2003), and nonspecific ion flux was defined either in the absence of agonist or in the presence of agonist (1 mM carbamylcholine) plus antagonist at a maximally effective inhibitory concentration (100 μM mecamylamine). Specific ion flux in test samples was calculated as the increase over nonspecific efflux and normalized as a percentage of specific efflux evoked by 1 mM carbamylcholine. Moreover, because some isotopic ion efflux occurred during the preincubation/desensitization period, not all cells retained the same amount of $^{86}Rb^+$ by the time that the assay for acute drug action was initiated. Accordingly, specific ion flux was further normalized

as a percentage of intracellular $^{86}Rb^+$ present at the beginning of the agonist-induced efflux period. There was no recovery time between the preincubation and agonist-induced efflux periods.

Concatemeric HS and LS $\alpha4\beta2$ Constructs. Human, fully pentameric $(\alpha4)_2(\beta2)_3$ (HS isoform; $\beta2$-$\alpha4$-$\beta2$-$\alpha4$-$\beta2$ subunit order) and $(\alpha4)_3(\beta2)_2$ (LS isoform; $\beta2$-$\alpha4$-$\beta2$-$\alpha4$-$\alpha4$ subunit order) concatemeric nAChR constructs were provided in the pCI oocyte expression vector by Isabel Bermudez (Oxford Brookes, Oxford, UK). These HS pentamer (HSP) and LS pentamer (LSP) constructs were as previously described (Carbone et al., 2009), except that each of the original native $\beta2$ subunit cDNA sequences were replaced with sequences optimized for expression in vertebrate expression systems (synthesized by GeneArt; Life Technologies, Grand Island, NY). The replacement $\beta2$ cDNA sequence encodes the native amino acid sequence, but it is optimized by minimization of high-GC content sequence segments, improved codon usage, reduction of predicted RNA secondary structure formation, and removal of sequence repeats and possible alternative start and splice sites.

As previously described (Carbone et al., 2009), the linkers between each subunit in the HSP and LSP cDNA constructs contain unique restriction sites that allow removal and replacement of individual subunits (see Fig. 1). As previously demonstrated, the initial $\beta2$-$\alpha4$ subunit protein pair of the LSP construct will assemble to form an orthosteric binding site between the complementary (−) face of the initial $\beta2$ subunit and the principal (+) face of the following $\alpha4$ subunit (Zhou et al., 2003). Accordingly, the assembled LSP (and HSP) $\alpha4\beta2$-nAChR proteins host orthosteric agonist binding pockets at the $\alpha4(+)/(-)\beta2$ interfaces between the first and second and the third and fourth, subunits. The recently discovered, LS-only $\alpha4(+)/(-)\alpha4$ interface thus forms between the (−) face of the $\alpha4$ subunit in LSP position 4, and the (+) face of $\alpha4$ subunit in position 5 (Harpsøe et al., 2011; Mazzaferro et al., 2011).

Canonical agonist binding pockets are predominantly formed from conserved residues from a set of three loops contributed by the (+) face of one α subunit (loops A–C), and by an additional loop contributed by the (−) face of the neighboring subunit (loop D, with smaller contributions from two further loops E and F) (Corringer et al., 2000; Brejc et al., 2002; Celie et al., 2004; Xiu et al., 2009). To assess the functional effects of mutating putative binding-pocket residues at the $\alpha4(+)/(-)\alpha4$ interface only present in the LSP construct (see Fig. 1), a set of six subunit mutants were synthesized (GeneArt; Life Technologies). Mutation of a set of conserved aromatic amino acids (tyrosines and tryptophans; to alanine in each case) in loops A–D was chosen (see Supplemental Fig. 1). Mutations in loops A–C were mapped to the (+)-face of the $\alpha4$ subunit in LSP position 5, whereas the loop D mutant mapped to the (−)-face of the $\alpha4$ subunit in LSP position 4 (Fig. 1). Each mutant subunit hosted one of the site-directed mutations together with the correct linker sequences and restriction sites to allow substitution for the target wild-type subunit within the LSP construct. Each aromatic residue that was mutated has been shown, by affinity labeling, X-ray crystallography, and/or site-directed mutagenesis, to have significant interactions with bound agonists at canonical nAChR agonist binding sites (Corringer et al., 2000; Brejc et al., 2002; Celie et al., 2004; Xiu et al., 2009). *S*ignal peptides were removed and replaced by linker peptides for all but the first subunit in each concatemer, but we used the conventional amino acid numbering scheme, starting with the translational initiation methionine as residue 1, and thus made the following mutations, all in the $\alpha4$ subunit: W88A (loop D), Y126A (loop A), W182A and Tyr184 (loop B), and Tyr223 and Tyr230 (loop C) (Fig. 2). For further context, the mutated $\alpha4(+)$ face residues correspond to Torpedo $\alpha1$ subunit conserved residues Tyr93 (loop A), Asp149 and Tyr151 (loop B), Tyr190 and Tyr198 (loop C), whereas the $\alpha4(-)$ mutation was performed at the residue corresponding to the conserved Asp55 or Asp57 of loop D in Torpedo γ or δ subunits, respectively.

The mutant subunits were then substituted for the corresponding-position wild-type subunits. Wild-type LSP in the pCI oocyte expression vector was restriction enzyme digested to remove the target subunit (XhoI and NotI for $\alpha4$ position 4, NotI and EcoRV for position 5; 2 hours at 37°C), the host construct was gel-purified, and the mutant subunit was ligated into the host. Correct substitution was confirmed using restriction digestion and by sequencing of the newly incorporated mutant $\alpha4$ subunits.

Concatemer RNA Preparation for Oocyte Injection. After plasmids were linearized with SwaI (2 hours at 37°C), treated with proteinase K (30 minutes at 50°C), and purified using Qiagen's PCR Clean-up Kit (Valencia, CA), cRNAs were transcribed using the mMessage mMachine T7 kit (Applied Biosystems/Ambion, Austin, TX). Reactions were treated with TURBO DNase (1 U for 15 minutes at 37°C) and cRNAs were purified using the Qiagen RNeasy Clean-up kit. cRNAs were confirmed on a 1% agarose gel and stored at −80°C.

Oocyte Preparation and RNA Injection. Methods of oocyte isolation and processing for receptor expression were previously described (Chang et al., 2002) but were modified as follows. *X. laevis* oocytes were purchased from Ecocyte LLC (Austin, TX) and were maintained at 13°C. The tips of pulled glass micropipettes were broken to achieve an outer diameter of approximately 40 μm (resistance of 2–6 MΩ), and pipettes were used to inject 80 nl containing 40 ng of RNA.

Two-Electrode Voltage-Clamp Determination of Concatemeric Construct Functional Expression in *X. laevis* Oocytes. Eight days after injection, oocytes expressing nAChR subunits were voltage clamped at −70 mV with an Axoclamp 900A amplifier (Molecular Devices, Sunnyvale, CA). Recordings were sampled at 10 kHz (low-pass Bessel filter: 40 Hz; high-pass filter: direct current), and the resulting traces were saved to disk (Clampex v10.2; Molecular Devices), and then extracted and analyzed using Clampfit software (Molecular Devices). Data from oocytes with leak currents (I_{leak}) >50 nA were excluded from recordings. Drugs were applied using a 16-channel, gravity-fed, perfusion system with automated valve control (AutoMate Scientific, Inc., Berkeley, CA) in oocyte Ringer's buffer (82.5 mM NaCl, 2.5 mM KCl, 1 mM $MgCl_2$, 1 mM $CaCl_2$, 1 mM Na_2HPO_4, 5 mM HEPES, supplemented with atropine sulfate 1.5 μM to block any possible muscarinic responses; pH = 7.5; OR2 buffer; flow rate = 4 ml min^{-1}). Postvalve tubing lengths were minimized, and a custom manifold was used to reduce dead volume, to optimize solution exchange at the oocyte (within the limitations imposed by the large size of a *X. laevis* oocyte). Typical valve openings were for 1 second (referred to henceforth as "1-second applications"). To obtain a practical measure of agonist pulse lengths as seen at the oocyte, 10 mM K^+ pulses (K^+ substituted for an equivalent amount of Na^+ in OR2 buffer) were applied directly to the oocyte. The resulting changes in membrane current under two-electrode voltage-clamp (TEVC) mode provided a receptor-independent measure of solution/oocyte contact time. Total application times after a 1-second valve opening were measured as 1.45 ± 0.04 seconds (measured from the beginning to the end of the deflection from baseline current), and peak application was 0.80 ± 0.02 seconds (measuring the time the response plateau was ≥90% of full K^+-induced deflection). Values in each case are the mean ± S.E.M. from four oocytes. In the case of A-85380 and Saz-A agonist acute application CRC experiments, the extremely low concentrations needed to define the lower part of the curve resulted in very slow response kinetics (presumably because of slow, diffusion rate–limited association of the agonist with the receptor). For agonist concentrations ≤10 nM, valve-open times were extended to 25 seconds to allow a full-peak response to develop.

[^{125}I]mAb295 Labeling of *X. laevis* Oocyte Surface LSP nAChR Populations. Mutations at the LSP construct $\alpha4/\alpha4$ interface could potentially contribute to changed functional expression by altering cell-surface expression levels. To determine whether this was the case, cell-surface nAChR expression levels were measured using [^{125}I]mAb295 binding assays. mAb295 is a monoclonal antibody raised against immunopurified chicken-brain nAChRs, and has been demonstrated to recognize specifically human, bovine, and rodent nAChR $\beta2$ subunits in native form (Whiting and Lindstrom, 1988; Lai et al., 2005; Whiteaker et al., 2006). Function of unmodified HSP and LSP, or variant LSP, constructs was first measured for individual

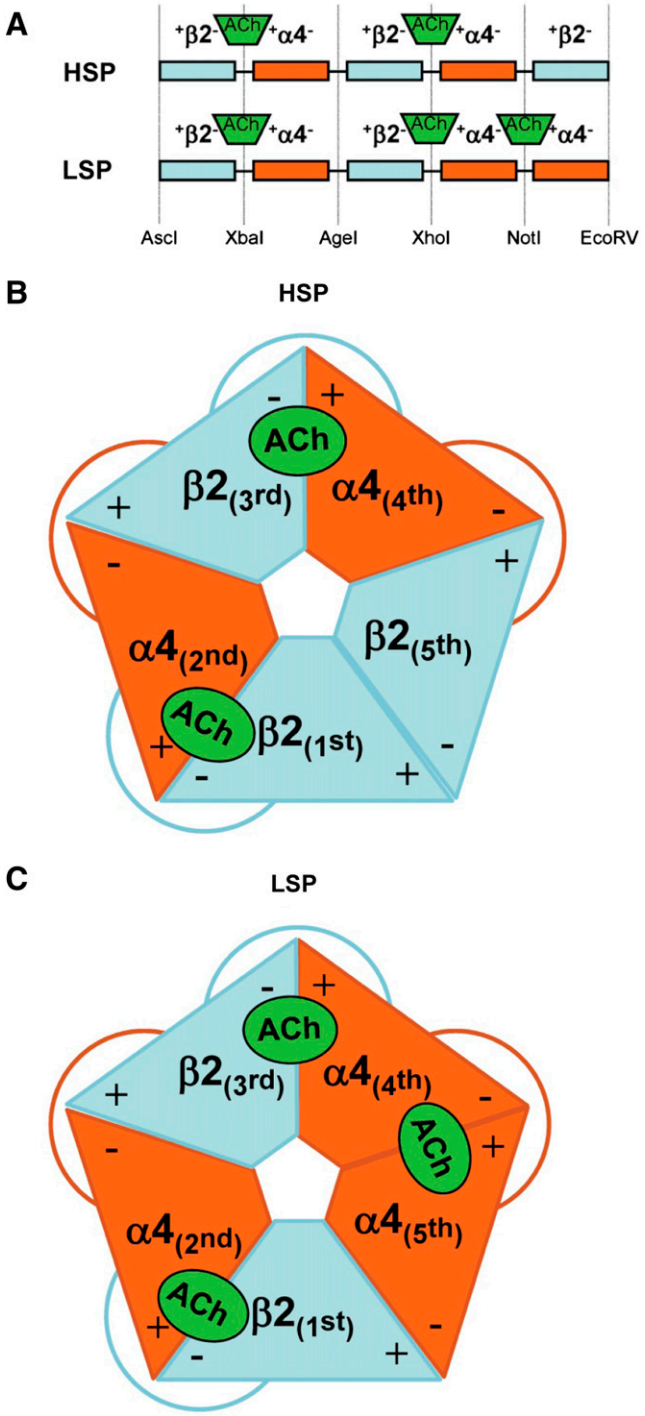

Fig. 1. Schematic diagrams of concatenated HS and LS α4β2-nAChR isoform pentameric constructs (HSP and LSP, respectively). (A) At the cDNA level, individual subunits are joined using linkers that encode AGS repeats. Each linker also contains a unique restriction site, noted at the base of (A). These sites allow rapid removal and replacement of individual subunits by a simple restriction digestion and ligation approach (Carbone et al., 2009). For both HSP and LSP, long-recognized agonist binding pockets form at the interfaces between the principal (+) faces of α4 subunits in positions 2 and 4, and the complementary (−) faces of β2 subunits in positions 1 and 3, respectively. The functional pharmacology implications of the further, LSP-unique, agonist binding pocket between the (+) face of α4 position 5 and the (−) face of α4 position 4 are explored in this study; site-directed mutant α4 subunits were substituted in positions 4 and 5 of the original LSP construct. (B) Schematic of an assembled HSP α4β2-nAChR, showing the arrangement of the subunit + and – interfaces, the resulting pair of agonist binding pockets, and the linkers. (C) Schematic of an assembled LSP α4β2-nAChR. Note that much of the structure is similar to the HSP isoform, but that an α4 subunit is substituted for the β2 subunit in position 5. This gives rise to the additional agonist binding site shown between the fourth and fifth subunits of LSP α4β2-nAChR.

oocytes, stimulated with a maximally effective ACh concentration (100 μM for HSP, 1 mM for LSP), using TEVC electrophysiology (see preceding description). β2-subunit–specific [^{125}I]mAb295 was then used essentially as previously described (Kuryatov and Lindstrom, 2011) to measure nAChR expression on the surface of the same oocytes. Oocytes were incubated for 3 hours in OR2 buffer supplemented with heat-inactivated normal horse serum [10%; to reduce nonspecific binding] and 2 nM β2-specific [^{125}I]mAb295 [a saturating concentration (Whiteaker et al., 2009)]. Unbound and nonspecifically bound [^{125}I]mAb295 was removed by three washes with ice-cold OR2 buffer (2 minutes each). Residual nonspecific binding was determined by incubating noninjected control oocytes in the same assay and subtracted from total binding to each test oocyte in order to calculate specific binding. Specific cell-surface binding of [^{125}I]mAb295 was converted to nAChR surface expression using the specific activity of the radiolabeled antibody and assuming two binding sites (i.e., β2 subunits) per LSP nAChR and three sites per HSP nAChR. The resulting nAChR expression data were then used to normalize concatemeric nAChR function.

Data Analysis. Maximum function (E_{max} for $^{86}Rb^+$ efflux, I_{max} for two-electrode voltage clamp) and log EC_{50}/IC_{50} values were determined from individual concentration-response experiments by nonlinear least-squares curve fitting (Prism 5.0; GraphPad Software, Inc., La Jolla, CA). Unconstrained monophasic or biphasic logistic equations were used to fit all parameters, including Hill slopes and fractional contributions of function attributable to HS or LS receptors, where applicable. Data were analyzed using the unpaired *t* test (two-tailed) to compare pairs of groups or by one-way or two-way analysis of variance (ANOVA) and Dunnett's multiple comparison test, to compare the means of three or more groups (Prism V5.0; GraphPad Software, Inc.).

Homology Modeling and ACh Docking. The amino-terminal domain of the human α4 nAChR subunit was aligned to the α7 nAChR chimera sequence from the crystal structure of 3SQ6, with extra residues at the sequence ends trimmed. The homology models of two α4 nAChR subunits were then built using ICM Pro 3.7 (Molsoft, San Diego, CA) with three-dimensional templates of chains A and B from the structure of 3SQ6. The resulting models were merged and optimized by ICM Pro software. Docking of ACh into the interface binding site of the homology model was performed with ICM Pro software. The docked result was presented with Discovery Studio Visualizer 3.0 (Accelrys, San Diego, CA).

Results

Acute Agonist Treatment in SH-EP1-hα4β2 Cells. We studied the properties of two nicotinic agonists that have previously demonstrated unusually high degrees of selectivity between HS and LS α4β2-nAChR: A-85380 and its derivative, Saz-A.

In SH-EP1-hα4β2 cells, acute exposure to Saz-A produced a potent, concentration-dependent ($\log EC_{50} = -8.70 \pm 0.07$; $n_H = 1.9 \pm 0.4$), monophasic, and apparently partial agonist response (E_{max} 55 ± 0.8% of the carbachol control in this set of experiments; Fig. 2A). Notably, the Saz-A concentration-response profile plateaus over at least four orders of magnitude. This contrasts with some agonists with efficacy that is likely limited by self-inhibition at higher drug concentrations and that yield bell-shaped CRCs.

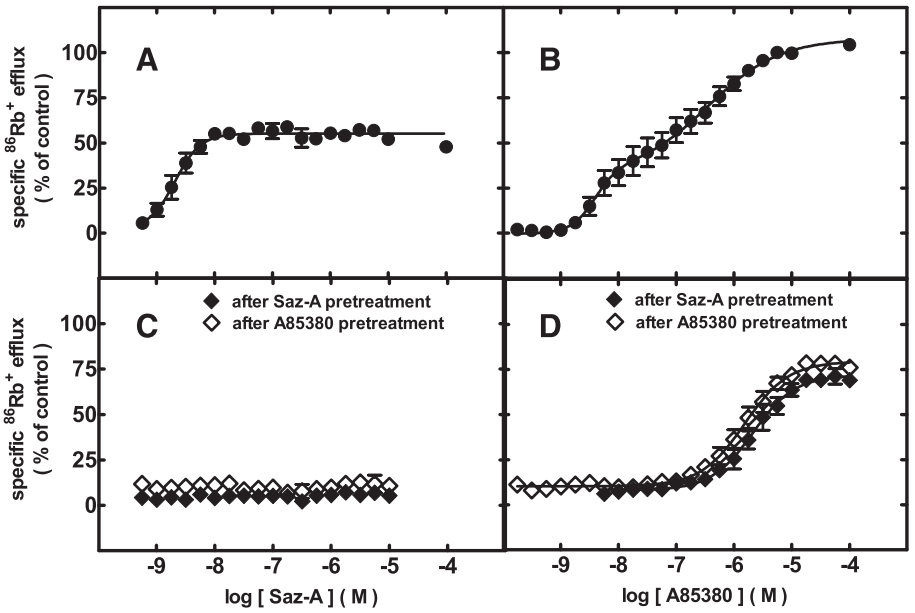

Fig. 2. Ligand-specific activation or desensitization of $\alpha4\beta2$-nAChR. SH-EP1-h$\alpha4\beta2$ cells stably expressing functional, human $\alpha4\beta2$-nAChRs from loose subunits were subjected to acute challenges for 5 minutes with the indicated drugs at the specified concentrations (abscissa; log M scale) for determination of specific $^{86}Rb^+$ efflux (defined in *Materials and Methods*) (ordinate; % of control response to a full agonist, 1 mM carbamylcholine). (A) Acute response to Saz-A (●). (B) Acute response to A-85380 (●). (C) Acute response to Saz-A after 10-minute pretreatment with 3.16 nM Saz-A (♦) or A-85380 (◇). (D) Acute response to A-85380 after 10-minute pretreatment with 3.16 nM Saz-A (♦) or A-85380 (◇). Results were fit to unconstrained, one- or two-site logistic equations. The derived $\log EC_{50}$ values, Hill coefficients, and fractional contributions of each site (in the case of two-site fits) are reported in the text.

By contrast to the monophasic, apparent partial, agonist activity shown by Saz-A, acute exposure to A-85380 produced a strongly biphasic CRC. Peak efficacy was comparable (108 ± 10%) to that of carbachol, the full-agonist control. Approximately 31 ± 18% or 69 ± 18% of function was seen in the HS and LS phases, respectively, in this set of experiments. Log EC_{50} values were −8.40 ± 0.14 and −6.44 ± 0.25, and n_H was 2.2 ± 1.6 and 0.7 ± 0.3 at the HS and LS isoforms, respectively (Fig. 2B). Note that curve fitting to five variables is inevitably subject to larger standard errors than for simpler concentration-response relationships.

Selective Desensitization of HS-Phase $\alpha4\beta2$-nAChR Function in SH-EP1-h$\alpha4\beta2$ Cells. We next defined the effects of 10-minute pretreatments with Saz-A or A-85380 on functional responses in SH-EP1-h$\alpha4\beta2$ cells subsequently subjected to acute agonist challenge. On the basis of the acute stimulation results (Fig. 3), pretreatment was performed using 3.16 nM ($10^{-8.5}$ M) Saz-A or A-85380. This concentration was determined in pilot studies to be sufficiently low as to produce submaximal activation of HS-phase $\alpha4\beta2$-nAChR function without activating LS-phase $\alpha4\beta2$-nAChR responses (in the case of A-85380). Concentration-response relationships were then defined for a 5-minute acute challenge with agonist, which was coapplied with the drug used in the pretreatment, without a recovery period.

Acute responses to Saz-A were essentially abolished after a 10-minute pretreatment with 3.16 nM Saz-A or 3.16 nM A-85380 (Fig. 2C). There was a small but measurable amount of $^{86}Rb^+$ efflux (≤10% of that for the full-agonist carbamylcholine control) in samples pretreated with 3.16 nM Saz-A or A-85380. This background level of function was due to steady-state efflux elicited by undissociated ligand bound during the pretreatment, and it was indistinguishable from the level of function observed in control experiments in which 3.16 nM drug pretreatments were followed by a treatment with buffer alone (data not shown, but this background level of function is evident from data at the lowest concentrations of drug used for acute challenge).

High concentrations of acutely applied A-85380 elicited functional responses from $\alpha4\beta2$-nAChRs in cells pretreated with the same 3.16 nM concentration of either Saz-A or A-85380 (Fig. 2D) that eliminated Saz-A–stimulated function. This is in strong contrast to the desensitization-induced full blockade of acute responses to Saz-A following the same pretreatment regimen. After Saz-A or A-85380 pretreatment, the remaining response to acutely applied high A-85380 concentrations closely resembled the LS $\alpha4\beta2$-nAChR component of function that was evoked by acute application of higher concentrations of A-85380 in non-pretreated cells. After pretreatment with 3.16 nM A-85380, the response to acute A-85380 was monophasic, with a $\log EC_{50}$ value of −5.82 ± 0.04, a Hill slope of 1.1 ± 0.1, and efficacy of 80 ± 2%. After pretreatment with 3.16 nM Saz-A, acute exposure to A-85380

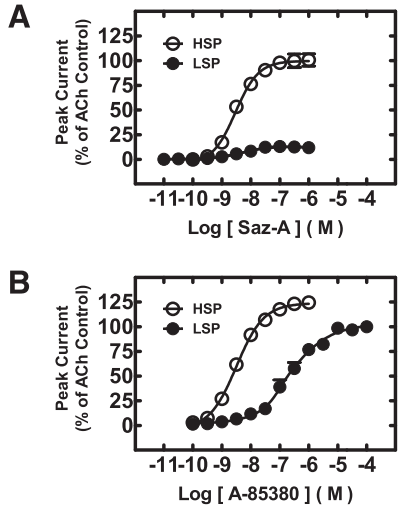

Fig. 3. Acute Saz-A and A-85380 stimulation of HSP versus LSP $\alpha4\beta2$-nAChR expressed in *X. laevis* oocytes. *X. laevis* oocytes expressing human HSP and LSP $\alpha4\beta2$-nAChR constructs were acutely stimulated with the indicated range of Saz-A (A) or A-85380 (B) concentrations. Values are the mean ± S.E.M. (n = 3 individual determinations), and are reported as the percentage of maximally efficacious ACh control responses (experimental details in *Materials and Methods*). Results were fit to unconstrained one-site logistic equations. The derived agonist $\log EC_{50}$, Hill coefficient, and efficacy values are reported in the text.

elicited function with an EC_{50} value of -5.68 ± 0.04, a Hill slope of 1.2 ± 0.2, and efficacy of $72 \pm 2\%$. Taking into account the approximately 10% background response during the 3.16 nM pretreatments, this indicates that a concentration of Saz-A (3.16 nM) that abolished HS-phase function reduced LS-phase function from 69 to 62% of control, a reduction of only 11%. The A-85380 pretreatment effect on A-85380–induced LS-phase function was even less pronounced. In neither case was evidence seen of HS $\alpha4\beta2$-nAChR–mediated responses superimposed above the previously noted background response (Fig. 2D). Thus, it appears that the same preapplied concentrations of Saz-A and A-85380 that strongly reduce HS-phase responses to either drug have little effect on LS-phase responses in the same cell line during 5-minute stimulation, as measured when using $^{86}Rb^+$ efflux.

Acute Saz-A and A-85380 Responses of HSP versus LSP $\alpha4\beta2$-nAChRs Expressed in *X. laevis* Oocytes. The results obtained in SH-EP1-h$\alpha4\beta2$ cells strongly suggested that pretreatment with Saz-A or A-85380 concentrations that greatly diminish HS-phase $\alpha4\beta2$-nAChR responses may induce significantly less loss of LS-phase $\alpha4\beta2$-nAChR function. We hypothesized that this was due to the recently discovered existence of a third binding site of lower affinity, at the $\alpha4(+)/(-)\alpha4$ interface (Harpsøe et al., 2011; Mazzaferro et al., 2011). However, attempting to disentangle effects in the SH-EP1-h$\alpha4\beta2$ cells' mixed HS and LS $\alpha4\beta2$-nAChR population could lead to errors of interpretation. To unequivocally study pure populations of HS or LS $\alpha4\beta2$-nAChRs, concatemeric constructs expressing functional $(\alpha4)_2(\beta2)_3$ and $(\alpha4)_3(\beta2)_2$ pentameric constructs (HSP and LSP, respectively; see Fig. 1) were used. We first subjected these populations to acute Saz-A and A-85380 stimulation, to test whether similar responses could be identified between the cell line–based and oocyte-based expression models. This was indeed the case. As illustrated in Fig. 3A, Saz-A produced a fully efficacious ($99 \pm 2\%$ of ACh control) and highly potent agonism ($\log EC_{50} = -8.53 \pm 0.06$) of HSP $\alpha4\beta2$-nAChR. In contrast, Saz-A efficacy at LSP $\alpha4\beta2$-nAChR was only $12 \pm 2\%$ of ACh control, although a very similar potency was observed at both $\alpha4\beta2$-nAChR isoforms (LSP $\log EC_{50} = -8.34 \pm 0.10$). Both CRCs were compatible with a single-site model, and produced similar Hill slopes (HSP Saz-A $n_H = 1.09 \pm 0.15$; LSP Saz-A $n_H = 1.02 \pm 0.23$). Acute A-85380 stimulation results were also compatible with the data obtained from the SH-EP1-h$\alpha4\beta2$ cell line, as shown in Fig. 3B. Although a small HS-phase response may be visible in the A-85380 activation trace, this could not reliably be fit using a two-site model. Because of this, data were fit to a single-site model, which calculated similar Hill slopes for each CRC (HSP A-85380 $n_H = 1.10 \pm 0.12$; LSP A-85380 $n_H = 0.93 \pm 0.11$). A-85380 was highly efficacious at both $\alpha4\beta2$-nAChR isoforms ($115 \pm 2\%$ efficacy compared with ACh control at HSP, $101 \pm 3\%$ at LSP), but was approximately 200-fold more potent at HSP versus LSP nAChR (HSP $\log EC_{50} = -8.55 \pm 0.05$; LSP $\log EC_{50} = -6.27 \pm 0.06$).

Differential Postdesensitization Responses of HSP versus LSP $\alpha4\beta2$-nAChR Concatemers Expressed in *X. laevis* Oocytes. For this and subsequent preincubation experiments, Saz-A was chosen since it has a simpler agonist profile (producing very little activation of LS-phase function, unlike A-85380; see the preceding section). Preincubation with 3.16 nM Saz-A reduced HSP $\alpha4\beta2$ I_{max} nAChR responses after acute exposure to a maximally effective ACh dose to $17.6 \pm 2.1\%$ of the control responses from oocytes that were not preincubated with Saz-A (Fig. 4). In contrast, $33.3 \pm 3.0\%$ LSP $\alpha4\beta2$-nAChR I_{max} function was retained under the same Saz-A (3.16 nM) preincubation conditions (Fig. 4). This difference was significant ($P < 0.01$; see the legend for Fig. 4).

The oocyte Saz-A desensitization experiments require repeated stimulation of the same oocyte with ACh (30 μM for HSP, 1 mM for LSP). ACh was chosen for these experiments because it is permanently charged, hydrophilic, and therefore easy to wash out of the test chamber. However, despite the 5-minute wash period between control and test stimulations, it was possible that test responses could be blunted by preceding control stimulations. This possibility was tested by washing with buffer alone, rather than buffer plus Saz-A, between ACh stimulations. In the absence of Saz-A, HSP $\alpha4\beta2$-nAChR test ACh responses were not reduced compared with preceding control responses (test response = $124 \pm 13\%$ of control; data not shown). The same outcome was found with responses recorded from LSP $\alpha4\beta2$-nAChR (test response = $109 \pm 15\%$ of control; data not shown). Thus, the loss in agonist response observed after Saz-A pretreatment was due only to Saz-A actions and not to desensitization induced by the initial control ACh stimulations used.

The $\alpha4(+)/(-)\alpha4$ Subunit Interface Forms an Agonist Binding Site That Is Required for Effective LSP $\alpha4\beta2$-nAChR Activation by Acute ACh Stimulation. HSP and LSP $\alpha4\beta2$-nAChRs share a pair of long-recognized agonist binding pockets, formed at the $\alpha4(+)/(-)\beta2$ subunit interfaces common to both $\alpha4\beta2$ isoforms (see Fig. 1). The ability of LS $\alpha4\beta2$-nAChRs to be stimulated by high agonist concentrations, even when the $\alpha4(+)/(-)\beta2$ sites are saturated (as

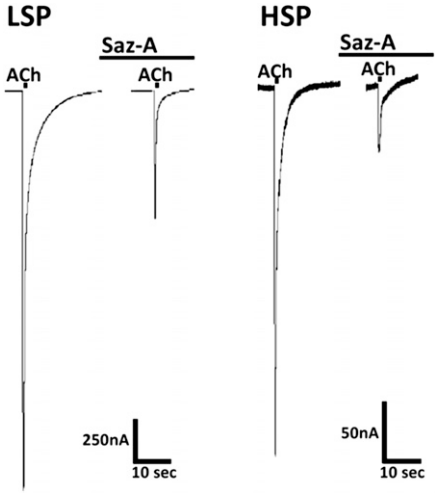

Fig. 4. Saz-A pretreatment effects on HSP versus LSP $\alpha4\beta2$-nAChR function. *X. laevis* oocytes injected with mRNA encoding either wild-type HSP $\alpha4\beta2$-nAChR or wild-type LSP $\alpha4\beta2$-nAChR were tested for the effects of Saz-A (5-minute) pretreatment on subsequent, acute, agonist stimulation. Initial control stimulation was performed for 1 second, using a maximally effective concentration of ACh (30 μM for HSP, 1 mM for LSP). Oocytes were then exposed to Saz-A (3.16 nM) for 5 minutes, and the ACh challenge was repeated (1-second stimulation, coapplied with 3.16 nM Saz-A); typical traces are shown. Saz-A pretreatment greatly reduced HSP responses (peak response diminished to $17.6 \pm 2.1\%$; mean ± S.E.M., $n = 4$). In contrast, Saz-A pretreatment diminished LSP peak responses to $33.3 \pm 3.0\%$ (mean ± S.E.M., $n = 4$). The difference in response to Saz-A pretreatment between HSP and LSP was significant (unpaired two-tailed t test, $t = 4.21$ with 6 degrees of freedom; $P < 0.01$).

demonstrated by loss of HSP responses), suggested that residual LS $\alpha4\beta2$-nAChR function might be activated by agonist binding to the $\alpha4(+)/(-)\alpha4$ subunit interface only found in the LS isoform (see *Materials and Methods* and Fig. 1). If so, mutation of critical residues within the $\alpha4(+)/(-)\alpha4$ site might be expected to reduce the relative amount of LS to HS function produced by $\alpha4\beta2$ LSP nAChR and/or to reduce the agonist potency for the LS phase of function. To test this hypothesis, a series of site-directed mutations were made to the $\alpha4(+)/(-)\alpha4$ subunit interface of the LSP construct. These mutations targeted highly conserved aromatic residues known to be involved in agonist binding across multiple nAChR subtypes (see *Materials and Methods* and Supplemental Fig. 1).

When an unmutated LSP $\alpha4\beta2$-nAChR population was acutely stimulated with ACh, 21 ± 3% of ACh-induced function fell into a HS phase, with an EC_{50} value very similar to that of an HS-isoform $(\alpha4)_2(\beta2)_3$-nAChR concatemeric construct (HSP; as shown in Fig. 5 and summarized in Table 1). This very closely resembles the 16% HS-like activity previously reported for LS $\alpha4\beta2$-nAChR [expressed using biased ratios of unlinked $\alpha4$ and $\beta2$ subunits (Harpsøe et al., 2011)]. The LS-phase function of the LSP construct had a $\log EC_{50}$ value of −4.39 ± 0.05 (or 41 μM). This was also very similar to the EC_{50} value (83 μM) recorded in the same study (Harpsøe et al., 2011), further confirming the suitability of the LSP construct as a model of LS $\alpha4\beta2$-nAChR function. As hypothesized, the HS-like proportion of function was significantly increased by mutations at the LSP $\alpha4(+)/(-)\alpha4$ subunit interface. This effect is shown in Fig. 5 (solid symbols), and summarized in Table 1. In addition, a subset of the mutated LSP mutants had significantly altered LS-phase EC_{50} values compared with the wild-type construct. Both constructs mutated in loop C showed a significant decrease in agonist potency (see Table 1). Surprisingly, ACh LS-phase potency was significantly higher at the loop B Y184A mutant compared with the unmodified LSP construct (Table 1), which may indicate that structure/function relationships at the $\alpha4(+)/(-)\alpha4$ site are not completely conserved compared with those reported at $\alpha4(+)/(-)\beta2$ agonist binding sites. Overall, these findings support the concept that conserved residues at the LSP $\alpha4(+)/(-)\alpha4$ subunit interface are critical for LS-phase function under acute stimulation conditions.

Pretreatment with Saz-A Eliminates the HS-Phase of ACh-Induced LSP Function, and Changes EC_{50} Values of LS-Phase Responses. Next, the same family of LSP constructs was pretreated with Saz-A (3.16 nM) for 5 minutes, before collection of ACh CRCs. The most dramatic effect of pretreatment was to reduce the HS-phase responses of all LSP variants to an undetectable level (Fig. 5, open symbols). This indicates that long-term agonist occupation of the conventional $\alpha4(+)/(-)\beta2$ agonist binding sites is sufficient to inactivate the HS-like phase of LSP function [which is therefore presumably mediated by the two $\alpha4(+)/(-)\beta2$ sites]. By extension, it might be expected that the equivalent sites in an HSP construct would be similarly affected by long-term Saz-A incubation. Because of this, any residual ACh-induced function would have to be produced via a minority of HSP nAChRs with unoccupied $\alpha4(+)/(-)\beta2$ sites. This should result in a smaller HSP response with no change in EC_{50} value (equivalent to the action of a noncompetitive antagonist). As shown in Fig. 6 and Table 1, this is exactly what was observed.

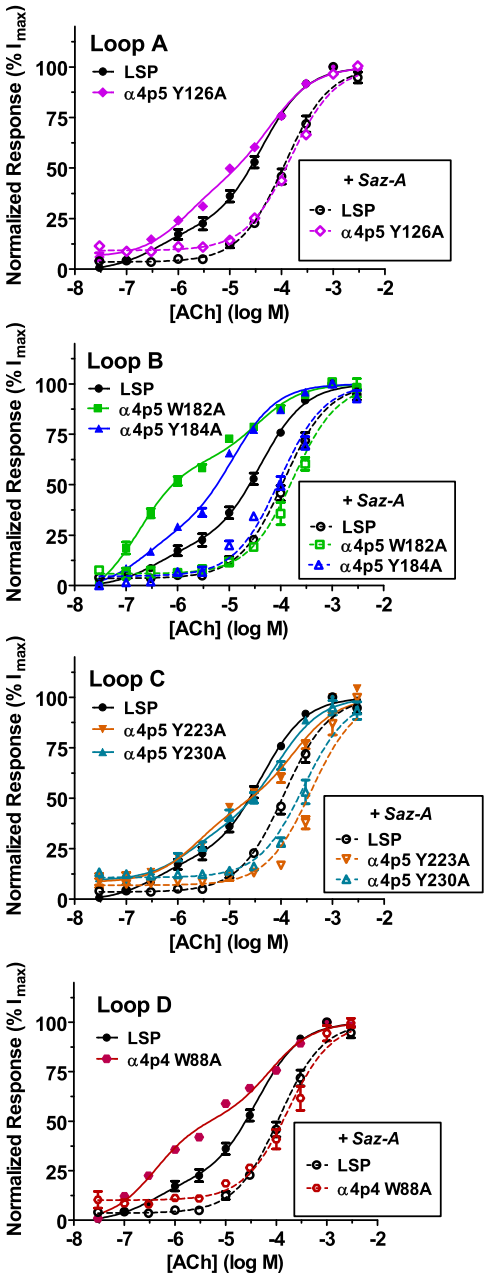

Fig. 5. ACh activation of wild-type versus mutant LSP $\alpha4\beta2$-nAChR. *X. laevis* oocytes injected with unmodified or mutant LSP mRNA were exposed to acute ACh challenges (1 second, concentrations specified on the *x* axis; log M scale). Filled symbols show concentration-response relationships determined for each LSP variant when exposed to acute ACh stimulation. Note that the proportion of HS-phase function is enhanced for every LSP mutant compared with the unmodified LSP construct. Open symbols depict concentration-response determinations for the same constructs, when exposed to a range of ACh concentrations after 5-minute preincubation with Saz-A (3.16 nM, 5 minutes). Pretreatment with Saz-A reduced HS-phase function of all LSP variants to such an extent that it could no longer be fit as part of a two-site model, leaving only LS-phase function. Log EC_{50} values for HS- and LS-phase responses, fractions of HS- versus LS-phase function, and statistical analyses are reported in Table 1. Points are the mean ± S.E.M. (n = 6–12).

Significantly, Saz-A occupation of the two LSP $\alpha4(+)/(-)\beta2$ agonist binding sites does change the EC_{50} of LS-phase responses (Fig. 6; Table 1). Thus, it seems that long-term occupation of the two $\alpha4(+)/(-)\beta2$ sites permits subsequent receptor activation through binding to the additional $\alpha4(+)/(-)\alpha4$ site

TABLE 1
Agonist stimulation parameters: ACh activation of unmodified versus mutant LSP $\alpha4\beta2$-nAChRs
All values are the mean ± S.E.M.

Concatemer	Mutation Site	ACh Only				ACh Post-Saz-A	
		Log (M) EC_{50} (HS)	HS Fraction	Log (M) EC_{50} (LS)	n	Log (M) EC_{50} (LS)	n
$\beta2$-$\alpha4$-$\beta2$-$\alpha4$-$\alpha4$ (LSP)	—	−6.44 ± 0.26	0.21 ± 0.03	−4.39 ± 0.05	12	−3.94 ± 0.03	8
$\beta2$-$\alpha4$-$\beta2$-$\alpha4^{W88A}$-$\alpha4$	Loop D	−6.39 ± 0.08	0.51 ± 0.02***	−4.13 ± 0.06	9	−3.77 ± 0.05	6
$\beta2$-$\alpha4$-$\beta2$-$\alpha4$-$^{Y126A}\alpha4$	Loop A	−5.87 ± 0.09	0.40 ± 0.03**	−4.21 ± 0.05	9	−3.83 ± 0.04	6
$\beta2$-$\alpha4$-$\beta2$-$\alpha4$-$^{W182A}\alpha4$	Loop B	−6.75 ± 0.08	0.65 ± 0.02***	−4.44 ± 0.08	9	−3.76 ± 0.05*	6
$\beta2$-$\alpha4$-$\beta2$-$\alpha4$-$^{Y184A}\alpha4$	Loop B	−6.68 ± 0.18	0.29 ± 0.03	−4.92 ± 0.05***	9	−4.05 ± 0.04	6
$\beta2$-$\alpha4$-$\beta2$-$\alpha4$-$^{Y223A}\alpha4$	Loop C	−5.62 ± 0.14*	0.42 ± 0.04***	−3.74 ± 0.08***	9	−3.42 ± 0.05***	6
$\beta2$-$\alpha4$-$\beta2$-$\alpha4$-$^{Y230A}\alpha4$	Loop C	−5.77 ± 0.21	0.29 ± 0.05	−4.06 ± 0.07*	9	−3.56 ± 0.05***	6
$\beta2$-$\alpha4$-$\beta2$-$\alpha4$-$\beta2$ (HSP)	—	−5.56 ± 0.04	1	—	5	−5.36 ± 0.05	8

Unmodified and mutant LSP construct mRNAs were expressed in *X. laevis* oocytes. ACh CRCs were performed either in the absence or presence of Saz-A preincubation (3.16 nM, 5 minutes). Oocytes were also injected with HSP mRNA for comparison with the LSP variants. Details are provided in the legend for Fig. 5 and in *Materials and Methods*. HS- and LS-phase $\log_{10}(EC_{50}/M)$, and fraction of HS-phase function were determined by least-squares curve fitting where possible (Saz-A preincubation rendered HS-phase function unmeasurable for all constructs). Numbers of individual oocytes tested are shown in the table (n = 6–12; derived from three separate experiments). Initially, two-way ANOVA was performed to determine the effect of mutation and treatment on the LS-phase EC_{50} values of the LSP construct ACh CRCs. Both factors significantly affected the observed EC_{50} values ($F_{6,28} = 53.8$, $P < 0.001$; and $F_{1,28} = 300$, $P < 0.001$, respectively), and a significant mutation × treatment interaction was also seen ($F_{6,28} = 6.54$, $P < 0.001$). For LS-phase EC_{50} values determined only with acute ACh exposure, ACh potency at the loop B Y184A mutant was significantly increased, whereas potency at the two C-loop mutants (Y223A and Y230A) was significantly reduced compared with the unmodified LSP control [one-way ANOVA with Dunnett's post hoc test ($F_{6,20} = 33.1$, $P < 0.001$)]. For residual LS-like responses measured after Saz-A preincubation, statistically significant decreases in ACh potency compared with the unmodified LSP control construct were observed for three mutants (one-way ANOVA with Dunnett's post hoc test $F_{6,20} = 24.0$, $P < 0.001$). The fraction of HS-phase function and ACh EC_{50} values for this function were determined before pretreatment with Saz-A (HS-phase responses were undetectable after pretreatment). A highly significant overall increase in the HS fraction was seen across the set of mutations (one-way ANOVA, $F_{6,20} = 22.8$, $P < 0.001$). Again, ACh potency was reduced compared with the unmodified LSP control construct by one of the C-loop mutants (Y223A; one-way ANOVA $F_{6,20} = 7.83$). *$P < 0.05$; **$P < 0.01$; ***$P < 0.001$ denote individual mutant differences from the control.

found only in LS $\alpha4\beta2$-nAChRs, but that this is accompanied by lowering of LS-phase agonist potency. Notably, the Saz-A–induced increase in the wild-type LS-phase ACh EC_{50} value as determined in these oocyte-electrophysiology experiments was very similar (approximately 1/2 log unit) to that previously seen in the $^{86}Rb^+$ experiments. As shown in Table 1, lower LS-phase agonist potency after Saz-A pretreatment is consistently observed across all of the $\alpha4(+)/(-)\alpha4$ site mutants produced for this study. However, the magnitude of the Saz-A–induced loss of LS-phase ACh potency varies between the mutants (i.e., a significant treatment × mutation interaction was observed; see legend to Table 1).

A possible alternative explanation for the lower LS-phase ACh potency in the presence of Saz-A could be that Saz-A interacts with low affinity with the $\alpha4(+)/(-)\alpha4$ site, acting as a weak competitive antagonist. This was tested for by measuring the LS-phase ACh EC_{50} value after 5-minute preincubation with a range of Saz-A concentrations. No systematic change in post-Saz-A LS-phase ACh EC_{50} value was observed, ruling out this possibility (at Saz-A concentrations of 1, 3.16, 10, and 31.6 nM; ACh logEC_{50} values were −4.13 ± 0.14, -−3.98 ± 0.04, −4.02 ± 0.06, and −4.00 ± 0.05, respectively; illustrated in Fig. 7A). Another significant observation is that for Saz-A concentrations ≥3.16 nM, the efficacy of LSP $\alpha4\beta2$-nAChR LS-phase responses to ACh shows no consistent change (at Saz-A concentrations of 3.16, 10, and 31.6 nM, maximum ACh-induced responses were 23.1 ± 1.7%, 14.3 ± 0.7%, and 18.2 ± 2.0% of the pre-Saz-A control, respectively). This plateau represents further evidence for a lack of Saz-A interaction at the $\alpha4(+)/(-)\alpha4$ site, even at the highest concentration tested (31.6 nM). In strong contrast, ACh-evoked responses at HSP $\alpha4\beta2$-nAChR were greatly reduced after pre-exposure to 1 nM Saz-A, and were undetectable after pre-exposure to 31.6 nM Saz-A (Fig. 7B).

Effects of $\alpha4(+)/(-)\alpha4$ site mutation on LSP HS-phase ACh EC_{50} values were also assessed (Table 1). Although HS-phase EC_{50} values were harder to measure precisely due to the generally smaller amounts of HS-phase function, a similar pattern emerged to that seen for the LS-phase: EC_{50} values trend lower for loop B mutants and higher for loop C mutants. However, a significant increase in HS-phase responses was only observed for the Y223A mutant (Table 1).

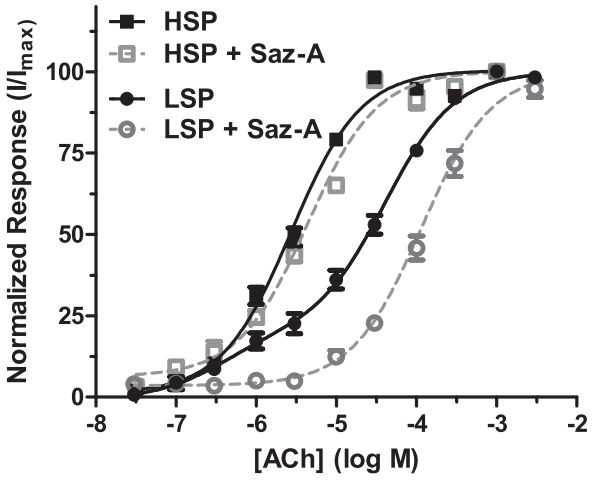

Fig. 6. Pretreatment with Saz-A eliminates the HS-phase of ACh-induced LSP function, and changes the EC_{50} of LS-phase responses. *X. laevis* oocytes injected with unmodified HSP (squares) and LSP (circles) mRNA were exposed to acute ACh challenges (1 second, concentrations specified on the x axis; log M scale), before (filled symbols) and after (open symbols) pretreatment with Saz-A (3.16 nM, 5 minutes). All concentration-response data are normalized to the maximum response measured for each concentration series, in each oocyte (mean ± S.E.M., n = 8–12). For HSP $\alpha4\beta2$-nAChRs, no change in ACh EC_{50} value was seen after preincubation with Saz-A. For LSP $\alpha4\beta2$-nAChRs, the HS-phase of the CRC (below approximately $10^{-5.5}$ M) was abolished by preincubation with Saz-A, whereas the potency of the LS-phase response was reduced. Log EC_{50} values for HS- and LS-phase responses, fractions of HS- versus LS-phase function, and statistical analyses are reported in Table 1.

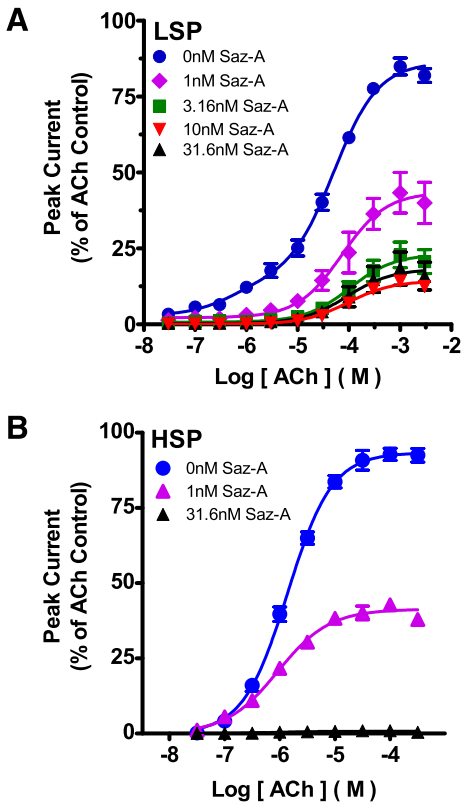

Fig. 7. Effects of changing Saz-A preincubation concentration on LSP and HSP ACh-induced responses. *X. laevis* oocytes injected with unmodified LSP (A) and HSP (B) mRNA were first exposed to a maximally effective ACh control challenge, followed by pretreatment with Saz-A (5 minutes, concentrations indicated in legends). Concentration-response data were then collected using a series of acute ACh challenges (1 second, concentrations specified on the *x* axis; log M scale, see *Materials and Methods* for details). All concentration-response data were normalized to the initial control stimulation, in each oocyte (mean ± S.E.M., $n = 3$). For LSP $\alpha4\beta2$-nAChR, Saz-A preincubation reduced (1 nM) and then abolished (> 3.16 nM) HS-phase responses. ACh EC_{50} values and magnitudes of LS-phase responses were unaffected by increasing Saz-A preincubation concentrations (3.16–31.6 nM; pharmacological parameters reported in the text). For HSP $\alpha4\beta2$-nAChRs, ACh responses were reduced by 1 nM Saz-A preincubation but, in contrast to LSP responses, no function remained after 31.6 nM Saz-A preincubation.

Effects of LSP $\alpha4(+)/(-)\alpha4$ Subunit Interface Mutations on Maximal ACh-Induced Function and Surface Expression. Mutation of the LSP $\alpha4(+)/(-)\alpha4$ interface greatly affected the maximum amount of function (I_{max}) that could be induced by ACh (Fig. 8A; note that the values shown in this panel are the sum of HS- and LS-phase function). Effects on I_{max} could again be segregated according to which agonist binding loop was mutated. Mutations in loops A (Y126A) or C (Y223A, Y230A) reduced I_{max} by >90% compared with the unmutated LSP construct. In contrast, mutations in loops B (W182A, Y184A) or D (W88A) reduced I_{max} by no more than approximately half. For comparison, I_{max} was also measured for oocytes expressing an HSP construct ($\beta2$-$\alpha4$-$\beta2$-$\alpha4$-$\beta2$), and was observed to be significantly lower than that produced by the related, and nonmutated, LSP construct ($\beta2$-$\alpha4$-$\beta2$-$\alpha4$-$\alpha4$). I_{max} values for each construct are summarized in Table 2.

The observed changes in I_{max} between LSP variants could be due to altered nAChR expression at the oocyte surface, altered amounts of function per unit of receptor, or a combination of both. Accordingly, we measured cell-surface nAChR expression using [^{125}I]mAb295 binding (Fig. 8B), for the same oocytes that were used in the I_{max} determinations. Note that, as described in *Materials and Methods*, we compensated for the different $\beta2$ subunit content of the HSP (3× $\beta2$ subunits per receptor) versus LSP constructs (2× $\beta2$ subunits per receptor). Mutation-induced differences in nAChR protein expression on the cell surface (summarized in Table 2) are much less pronounced than are the accompanying changes in I_{max}. In fact, although a trend can be observed toward lower surface expression by constructs harboring loop A and C mutant subunits, one-way ANOVA showed no significant differences compared with the unmodified LSP control (Table 2). Despite this apparent trend, when I_{max} was normalized per unit of cell-surface nAChR protein expression (Fig. 8C; Table 2), significant reductions in per-receptor I_{max} were still noted for the LSP loop A and C mutants compared with the unmodified LSP constructs. However, I_{max} per receptor was not significantly changed by mutations in the B or D loops. These outcomes closely mirror the findings regarding I_{max} only, demonstrating the dominant role of changes in "per-receptor" function, as opposed to changes in surface expression, in mediating overall changes in I_{max}.

By combining the normalized I_{max} values with HS-fraction data from Table 1, it was possible to calculate the absolute amounts of HS-phase and LS-phase function per unit of cell-surface nAChR expression (Fig. 8C, black portions of the histogram show HS-phase function, white portions show LS-phase function). Strikingly, two mutants produced increased HS-phase function (W88A in loop D, W182A in loop B). For all other mutants, there was a trend toward reduced HS-phase function, although this did not quite reach significance (one-way ANOVA). Even more interestingly, I_{max}/fmol surface-expressed receptor was indistinguishable between the HS phase of the unmodified LSP construct and the HSP construct (which produces only HS-phase function).

Part of the I_{max} response to acute ACh stimulation is mediated by HS-phase function, which is lost after Saz-A treatment. Data from this study indicate that any agonist-induced LS-phase response of LSP nAChRs is produced by an agonist interaction at the $\alpha4/\alpha4$ site. This is true whether the $\alpha4/\beta2$ sites are occupied long term by a selective compounds such as Saz-A, or not (as in the case of a simple acute agonist challenge). Given this observation, it is arguably more legitimate to compare the magnitude of post-Saz-A responses to only the LS phase of the corresponding pre-Saz-A responses. For instance, 21% of the pre-Saz-A LSP I_{max} response shown in Fig. 4 is produced by HS-phase current. Thus, LS-phase function represents only 79% of the LSP I_{max}. When the maximum response is reduced after Saz-A pretreatment to 33% of the pre-Saz-A LSP I_{max} control, given the elimination of the 21% contribution from the HS phase, there is a 58% reduction in the LS phase of the response due to Saz-A pretreatment. Residual LS-only peak function thus corresponds to 42% of the original LS-phase peak response. As shown in Fig. 9, the reduction in LS-phase function after Saz-A (3.16 nM) pretreatment is not significantly different across the set of LSP variants tested in this study (although several mutants appeared to show a trend toward a larger proportion of function retained).

Discussion

The principal novel observation from this study is that preapplication of compounds that selectively interact with $\alpha4$

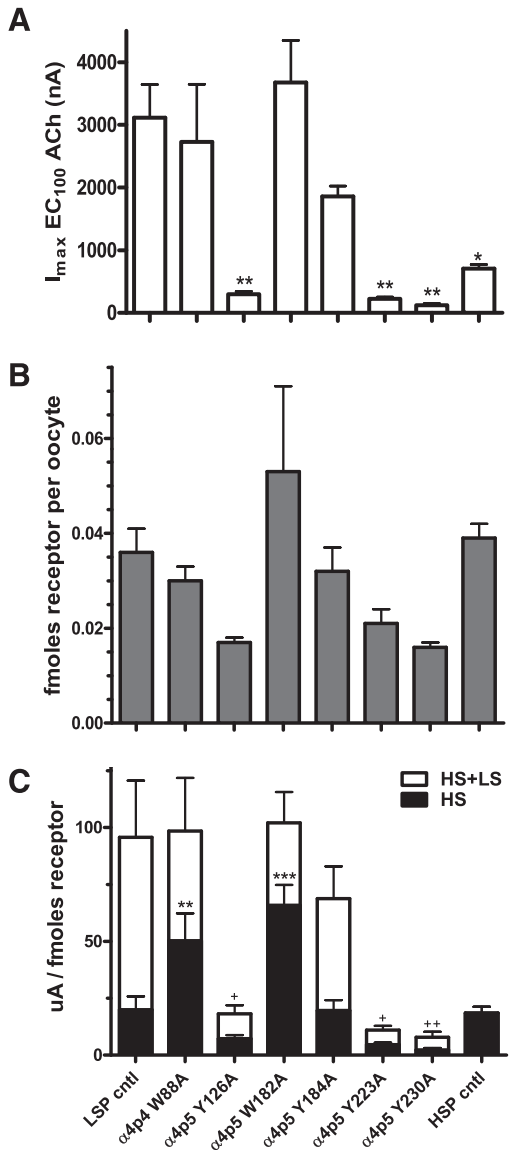

Fig. 8. LSP $\alpha4(+)/(-)\alpha4$ interface mutation effects on maximum peak ACh-induced function (I_{max}) and nAChR cell-surface expression. *X. laevis* oocytes were injected with mRNAs encoding either unmodified or mutant LSP constructs (loop A, Y126A; loop B, W182A and Y184A; loop C, Y223A and Y230A; loop D, W88A), or an unmodified HSP construct (see *Materials and Methods* for details). (A) Maximum peak ACh-induced function (I_{max}) was determined for each construct. I_{max} is significantly reduced by several of the mutations compared with the unmodified LSP construct, and the HSP construct also has a significantly lower I_{max} value than that recorded for the wild-type LSP construct. $^{*}P < 0.05$; $^{***}P < 0.001$. (B) nAChR protein expression at the surface of *X. laevis* oocytes was determined using an [^{125}I]mAb295 binding assay. To note, binding of two [^{125}I]mAb295 molecules per LSP construct and three per HSP construct (reflecting the different $\beta2$ subunit numbers in each nAChR isoform; see *Materials and Methods*) was assumed. Although some apparent variation in nAChR cell-surface expression was observed across the tested constructs, this did not reach the level of statistical significance. (C) I_{max} values were normalized to the amounts of nAChR cell-surface expression for each construct. By applying the HS-phase function fractions calculated for each construct (Table 1), it was possible to determine the absolute amount of HS- and LS-phase function for each construct. Significant changes are noted as follows: $^{**}P < 0.01$; $^{***}P < 0.001$ for HS-phase function; and $^{+}P < 0.05$; $^{++}P < 0.01$ for overall function (I_{max}). To note, the HSP result was not included in the overall function comparison for (C), since this construct produces only HS-phase function. Details of the analysis applied, and parameter values determined, are supplied in Table 2.

$(+)/\beta2(-)$ agonist binding sites preferentially diminishes HS-phase versus LS-phase $\alpha4\beta2$-nAChR function. Our results also show that the recently discovered $\alpha4(+)/(-)\alpha4$ subunit interface agonist binding site uniquely found in the LS isoform (Fig. 1) underlies this differential functional outcome. Since $\alpha4\beta2$ is the predominant neuronal nAChR subtype, these discoveries are likely to have significant functional implications and to provide important insights for drug discovery and development efforts.

The current findings concerning acute responses to A-85380 and Saz-A are consistent with previous reports. A-85380 agonist action at $\alpha4\beta2$-nAChRs was previously shown to have a biphasic concentration-response relationship with >100-fold higher potency at HS than LS $\alpha4\beta2$-nAChRs, and similar efficacy in both populations (Marks et al., 1999; Carbone et al., 2009). Similarly, our acute Saz-A stimulation data are consistent with prior observations that Saz-A is a full agonist at heterologously expressed HS receptors and is poorly efficacious at $\alpha4\beta2$-nAChRs (Zwart et al., 2008; Kozikowski et al., 2009). We demonstrate for the first time, using both loose-subunit and concatemeric approaches, that pretreatment with a low concentration of either A-85380 or Saz-A essentially abolishes HS-phase $\alpha4\beta2$-nAChR responses to subsequent acute agonist applications. In contrast, the same pretreatment only induces a partial loss of subsequent LS-phase $\alpha4\beta2$-nAChR agonist responses. This contrasts with a previous study that indicated similar HS versus LS desensitization potencies for a range of other nicotinic agonists (Marks et al., 2010). The differences between our findings and those of Marks et al. (2010) likely reflect the exceptional HS-$\alpha4\beta2$ versus LS-$\alpha4\beta2$ selectivity of A-85380 and Saz-A, presumably due to their strong preference for $\alpha4(+)/(-)\beta2$ over $\alpha4(+)/(-)\alpha4$ subunit agonist binding pockets.

Notably, function that was identified as being LS-like in SH-EP1-h$\alpha4\beta2$ cells was only reduced by 11% after extended exposure to 3.16 nM Saz-A, whereas a greater effect was seen on LS-phase function of LSP nAChRs expressed in *X. laevis* oocytes. To some extent, this may reflect the uncertainty inherent in using least-squares curve fitting to separate HS from LS $\alpha4\beta2$-nAChR function in the cell line's mixed population. In addition, it is important to note that $(\alpha4)_3(\beta2)_2$-nAChR function contains an intrinsic component of HS-like activity. Because of this, the reported 67% loss of LSP I_{max} function measured in the oocyte experiments overestimates the effect of Saz-A pretreatment on the LS-only phase of function. Much of this difference is, however, likely due to the fact that peak inward current responses were measured in the oocyte-electrophysiology experiments, whereas integrated function over 5 minutes was measured in the cell line $^{86}Rb^{+}$ experiments. Because of this, it seems likely that the two isoforms will be differentially affected by synaptically released brief pulses of high concentration ACh (which will activate both isoforms) as opposed to by interaction with interstitial, volume transmitted ACh and/or exogenous nicotinic compounds. In the latter case, compounds will be present at much lower concentrations, and may also be present for significantly longer time scales than intrasynaptic ACh. Accordingly, the $^{86}Rb^{+}$ efflux measurements may be more applicable to the extrasynaptic context, in which cumulative function from longer-term stimulation may predominate over peak function. However, the central finding was that, in both the cell line and oocyte experiments, across widely different

TABLE 2
Effects of $\alpha4(-)/(+)\alpha4$ agonist binding site mutations on LSP construct function and cell-surface expression
All values are the mean ± S.E.M.

Concatemer	Mutation Site	ACh I_{max}	Specific [^{125}I]mAb 295 Binding	n	HS Phase	LS Phase
		nA	*fmol/oocyte*		*μA/fmol*	*μA/fmol*
$\beta2$-$\alpha4$-$\beta2$-$\alpha4$-$\alpha4$ (LSP)	—	3100 ± 530	0.036 ± 0.005	5	19.9 ± 5.8	75.7 ± 19.8
$\beta2$-$\alpha4$-$\beta2$-$\alpha4^{W88A}$-$\alpha4$	Loop D	2700 ± 920	0.030 ± 0.003	3	50.2 ± 12.1**	48.1 ± 11.4
$\beta2$-$\alpha4$-$\beta2$-$\alpha4^{Y126A}\alpha4$	Loop A	300 ± 50**	0.017 ± 0.001	3	7.2 ± 1.6	10.9 ± 2.3*
$\beta2$-$\alpha4$-$\beta2$-$\alpha4^{W182A}\alpha4$	Loop B	3700 ± 670	0.053 ± 0.018	3	65.8 ± 9.0***	36.2 ± 4.8
$\beta2$-$\alpha4$-$\beta2$-$\alpha4^{Y184A}\alpha4$	Loop B	1900 ± 170	0.032 ± 0.005	3	19.7 ± 4.5	49.1 ± 10.2
$\beta2$-$\alpha4$-$\beta2$-$\alpha4^{Y223A}\alpha4$	Loop C	220 ± 30**	0.021 ± 0.003	3	4.6 ± 0.9	6.4 ± 1.1*
$\beta2$-$\alpha4$-$\beta2$-$\alpha4^{Y230A}\alpha4$	Loop C	120 ± 30**	0.016 ± 0.001	3	2.3 ± 0.8	5.5 ± 1.7**
$\beta2$-$\alpha4$-$\beta2$-$\alpha4$-$\beta2$ (HSP)	—	710 ± 60*	0.039 ± 0.003	3	18.4 ± 2.8	Not applicable

Unmodified and mutant LSP, and HSP, nAChR construct mRNAs were expressed in *X. laevis* oocytes. ACh CRCs were performed in the absence of Saz-A preincubation. Maximum function (I_{max}) and the fraction of HS-phase function were determined by least-squares curve fitting. Surface expression of nAChR was then determined for the same oocytes using [^{125}I]mAb295 binding (see *Materials and Methods*). Data were collected from three to five individual experiments, with six oocytes tested per condition in each experiment. One-way ANOVA was used to test within each measure for differences from control (unmodified LSP) parameters, with Dunnett's post hoc test used to identify individual constructs that differed from control. Overall ANOVA results showed significant differences in overall I_{max} (sum of HS- and LS-phase function; $F_{7,17} = 8.43$, $P = 0.0002$), and also in surface expression levels ($F_{7,17} = 3.101$, $P = 0.025$, although post hoc testing failed to identify differences versus the unmodified LSP control for the HSP or for any of the mutant LSP constructs). Overall (I_{max}) function was subdivided into HS- and LS-phase responses for each construct where possible (no LS-phase function was produced by HSP nAChRs), and normalized to nAChR surface expression levels. Significant differences were seen in both normalized HS-phase function ($F_{7,17} = 12.6$, $P < 0.0001$; two constructs showed increased HS-phase function) and in normalized LS-phase function ($F_{6,16} = 4.57$, $P = 0.0069$; all constructs showed a trend to decreased LS-phase function, with three reaching statistical significance). *$P < 0.05$; **$P < 0.01$; ***$P < 0.001$.

timescales, significantly more LS-phase versus HS-phase $\alpha4\beta2$-nAChR function was retained after exposure to the same concentration of Saz-A.

Our observations confirm the recent finding (Harpsøe et al., 2011) that approximately 20% of LS-isoform $\alpha4\beta2$-nAChR function induced by ACh occurs in an HS-like phase. Whether HS $(\alpha4)_2(\beta2)_3$ versus LS $(\alpha4)_3(\beta2)_2$ stoichiometry is enforced using either biased subunit expression ratios or linked-subunit approaches, HS functional expression is consistently lower than that of LS $\alpha4\beta2$-nAChRs (Zwart and Vijverberg, 1998; Nelson et al., 2003; Zhou et al., 2003; Carbone et al., 2009; Harpsøe et al., 2011; Mazzaferro et al., 2011). In this study, we show for the first time that both isoforms express equally well at the cell surface. However, maximum function is approximately five times greater on a "per-receptor" basis for LS- versus HS-isoform $\alpha4\beta2$-nAChRs (Fig. 8C). Interestingly, the HS/LS functional ratio is close to 1:1 across all mouse brain regions (Marks et al., 1999). This implies that the majority (approximately 80%) of naturally expressed $\alpha4\beta2$-nAChRs are of the $(\alpha4)_2(\beta2)_3$ stoichiometry, confirming earlier conclusions (Anand et al., 1991; Cooper et al., 1991). It is important to note that although HS/LS $\alpha4\beta2$-nAChR functional ratios are similar across multiple brain regions, this does not necessarily mean that distributions of the isoforms are similar at the cellular or circuit level. In fact, observations of differing effects across multiple $\alpha4\beta2$-nAChR–mediated behavioral measures for the LS isoform–selective positive allosteric modulator 3-[3-(pyridin-3-yl)-1,2,4-oxadiazol-5-yl]benzonitrile (NS9283) (Timmermann et al., 2012) imply that this is not the case.

Intriguingly, the HS-phase response of LSP $\alpha4\beta2$-nAChRs is indistinguishable in magnitude from that of the total HSP response, on a per-receptor basis. This suggests that, for acute agonist stimulations, recruitment of the $\alpha4(+)/(-)\alpha4$ site at higher agonist concentrations acts to boost what would otherwise be similar function, mediated by the pair of $\alpha4(+)/(-)\beta2$ sites shared by both isoforms. Agonists binding at the $\alpha4(+)/(-)\alpha4$ site could, therefore, be considered to act similarly to positive allosteric modulators. In fact, Zn^{2+} has already been shown to be an allosteric activator of LS $\alpha4\beta2$-nAChR by binding to different residues within the $\alpha4(+)/(-)\alpha4$ interface than those probed here (Moroni et al., 2008). After long-term occupation of $\alpha4(+)/(-)\beta2$ sites by selective agonists such as A-85380 or Saz-A, it would seem likely that both HS and LS $\alpha4\beta2$-nAChR isoforms will become desensitized. The LS-phase responses evoked by subsequent agonist challenges at LS-isoform $\alpha4\beta2$-nAChRs would, in this understanding, be due to a reactivation of the desensitized LS-isoform nAChRs through the previously unbound $\alpha4(+)/(-)\alpha4$ site. In a further point of similarity, this could be considered to be analogous to the previously reported activity of some positive allosteric modulators at $\alpha7$ nAChRs (Grønlien et al., 2007; Williams et al., 2011).

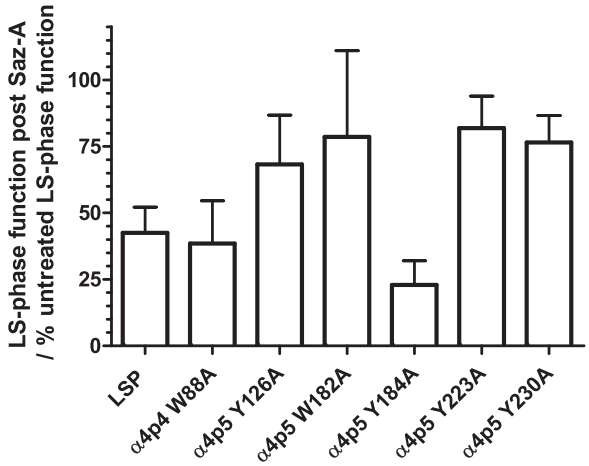

Fig. 9. Comparison of Saz-A pretreatment effects on LS-phase function across LSP variants. *X. laevis* oocytes were injected with unmodified and mutant LSP mRNAs. ACh concentration-response experiments were performed to determine maximal LS-phase function before and after pretreatment with Saz-A (3.16 nM, 5 minutes). The percentage of post-treatment versus pretreatment LS-phase function is displayed for each LSP variant construct used in this study. Values are the mean ± S.E.M. of 6–8 individual determinations collected from three separate experiments. One-way ANOVA showed no significant differences across the LSP variants ($F_{6,14} = 1.85$; $P = 0.16$).

The presence of a third, functionally important, agonist site in a heteromeric nAChR is a relatively novel finding. However, this concept fits with findings regarding other members of the cystine loop, LGIC superfamily. Of direct relevance, the $\alpha1\beta-$ glycine receptor assembles with an $(\alpha1)_3(\beta)_2$ subunit stoichiometry (Kuhse et al., 1993; Burzomato et al., 2003), and also seems to possesses three functionally relevant agonist binding sites (Burzomato et al., 2004). Furthermore, two of these sites are likely located at earlier-identified $\alpha1/\beta$ subunit interfaces, but the third site is likely located at the $\alpha1/\alpha1$ subunit interface, directly analogous to the nAChR $\alpha4(+)/(-)\alpha4$ subunit interface. Importantly, maximally effective activation of homomeric $\alpha7$/5-HT3 chimeric receptors also requires activation of three agonist binding sites of the five available (Rayes et al., 2009). Additional, although less directly analogous, examples are provided by allosteric activators of LGICs. For $GABA_A$ receptors, benzodiazepine allosteric actions are known to be mediated through drug interactions with a noncanonical α and γ subunit interface site (Sigel and Buhr, 1997). In addition, the partial agonist, morantel, potentiates acetylcholine-induced responses of $\alpha3\beta2$-nAChRs (Seo et al., 2009). The interpretation was that morantel interacts at noncanonical $\beta2(+)/(-)\alpha3$ interfaces, which would be analogous to nAChR $\beta2(+)/(-)\alpha4$ interfaces in the $\alpha4\beta2$ isoforms. Regardless of the fidelity with which functional and structural features of the recently discovered $\alpha4(+)/(-)\alpha4$-interface agonist binding site in LS $\alpha4\beta2$-nAChRs match those in other LGICs, the existence of additional functionally important subunit-interface binding sites (outside of the set of long-recognized agonist binding pockets) seems to generalize across the LGIC superfamily.

Use of the LSP $\alpha4\beta2$-nAChR construct enabled site-directed mutagenesis of critical residues only at the putative $\alpha4(+)/(-)\alpha4$ agonist binding pocket. This level of precision would not have been available if a nonlinked subunit approach had been employed. The most notable and consistent effect of such mutations was to increase the ratio of HS- to LS-phase function compared with the unmodified LSP control (Fig. 5; Table 1). This observation is consistent with previous work (Mazzaferro et al., 2011), although that study failed to note the presence of an intrinsic HS-phase component within the wild-type $(\alpha4)_3(\beta2)_2$ response. Compared with the often-dramatic effects on LS-phase efficacy, mutation-induced changes in agonist LS-phase potency were relatively minor. This is also consistent with earlier work (Galzi et al., 1991) in which several equivalent residues were altered in $\alpha7$ nAChRs. Despite the fact that these mutations were introduced into five binding pockets (compared with only one here), most EC_{50} and IC_{50} shifts for competitive ligands were also quite limited (approximately 10-fold or less). The surprising increase in LS-phase ACh potency for our Y184A mutant, however, suggests that there may be some fundamental structure/function differences between the recently discovered $\alpha4(+)/(-)\alpha4$ site and previously recognized agonist binding pockets. Such differences may prove useful for drug discovery/development work.

Our findings indicate a degree of functional interdependence between the pair of $\alpha4(+)/(-)\beta2$ sites and the $\alpha4(+)/(-)\alpha4$ site within each LS $\alpha4\beta2$-nAChR. For example, the per-receptor amount of HS-phase function [presumably mediated by the $\alpha4(+)/(-)\beta2$ sites] can be decreased or even increased by individual mutations at the $\alpha4(+)/(-)\alpha4$ site. Conversely, persistent Saz-A occupation of the $\alpha4(+)/(-)\beta2$ sites reduces the efficacy and potency of LS $\alpha4\beta2$-nAChR activation via the $\alpha4(+)/(-)\alpha4$ site. Determining the precise interplay between the three agonist sites within the LS isoform will likely require a great deal of further analysis, but should yield fundamental insights into activation mechanisms for both nAChR and the wider LGIC superfamily.

The existence of HS and LS $\alpha4\beta2$-nAChR isoforms has been known for over a decade. However, the relative distributions of HS and LS $\alpha4\beta2$-nAChR isoforms within brain regions and across neuronal structures, as well as their physiologic roles, are not well understood. The results presented here illuminate receptor-level differences that underlie the differential pharmacology of the two $\alpha4\beta2$-nAChR isoforms. Our findings also illustrate that it is possible to selectively manipulate HS versus LS $\alpha4\beta2$-nAChR activity using pharmacological approaches. The unique, $\alpha4(+)/(-)\alpha4$ interface, ligand-binding site of LS $\alpha4\beta2$-nAChR provides novel drug design opportunities. Examples could include competitive antagonists to selectively block LS $\alpha4\beta2$-nAChR, agonists to selectively activate LS receptors, or compounds to "prime" LS receptors to effectively exhibit HS-like responses to endogenous acetylcholine. Such pharmacological tools could be used to uncover the physiologic roles of HS versus LS $\alpha4\beta2$-nAChRs. The compounds used in this study (A-85380 and Saz-A) may serve as useful lead molecules for the discovery of further HS versus LS $\alpha4\beta2$-nAChR selective compounds. As the predominant neuronal nAChR subtype, $\alpha4\beta2$-nAChRs are prominent targets for drug development and of existing smoking cessation therapies. Effects of existing compounds on HS and LS $\alpha4\beta2$-nAChR isoforms often are not well characterized. However, the balance of activation/inactivation of HS- versus LS-phase $\alpha4\beta2$-nAChR function could be extremely important. Success in creation of superior aids to smoking cessation and new nicotinic drugs for treatment of neurologic or psychiatric disorders involving $\alpha4\beta2$-nAChRs may depend on the selectivity of drug interactions with HS and LS $\alpha4\beta2$ isoforms.

Acknowledgments

The authors thank Drs. F. Ivy Carroll (Research Triangle Institute, Research Triangle Park, NC) and Alan P. Kozikowski (University of Illinois, Chicago, IL) for gifts of compounds and Dr. Isabel Bermudez (Oxford Brookes University, Oxford, UK) for providing the original HSP and LSP $\alpha4\beta2$ constructs that were modified for use in this study. The authors also thank Robert A. Ellingford (a placement student at the University of Bath, Bath, UK) and Dr. Andrew George (a research assistant professor at Barrow Neurologic Institute, Phoenix, AZ) for excellent technical assistance.

Authorship Contributions

Participated in research design: Eaton, Lucero, Stratton, Chang, Cooper, Lindstrom, Lukas, Whiteaker.

Conducted experiments: Eaton, Lucero, Stratton, Whiteaker.

Contributed new reagents or analytic tools: Cooper, Lindstrom.

Performed data analysis: Eaton, Lucero, Stratton, Chang, Lukas, Whiteaker.

Wrote or contributed to the writing of the manuscript: Eaton, Lucero, Chang, Lindstrom, Lukas, Whiteaker.

References

Abreo MA, Lin NH, Garvey DS, Gunn DE, Hettinger AM, Wasicak JT, Pavlik PA, Martin YC, Donnelly-Roberts DL, and Anderson DJ, et al. (1996) Novel 3-Pyridyl ethers with subnanomolar affinity for central neuronal nicotinic acetylcholine receptors. *J Med Chem* **39**:817–825.

Anand R, Conroy WG, Schoepfer R, Whiting P, and Lindstrom J (1991) Neuronal nicotinic acetylcholine receptors expressed in Xenopus oocytes have a pentameric quaternary structure. *J Biol Chem* **266**:11192–11198.

Brejc K, van Dijk WJ, Smit AB, and Sixma TK (2002) The 2.7 angstrom structure of AChBP, homologue of the ligand-binding domain of the nicotinic acetylcholine receptor. *Novartis Found Symp* **245**:22–29, discussion 29–32, 165–168.

Burzomato V, Beato M, Groot-Kormelink PJ, Colquhoun D, and Sivilotti LG (2004) Single-channel behavior of heteromeric alpha1beta glycine receptors: an attempt to detect a conformational change before the channel opens. *J Neurosci* **24**: 10924–10940.

Burzomato V, Groot-Kormelink PJ, Sivilotti LG, and Beato M (2003) Stoichiometry of recombinant heteromeric glycine receptors revealed by a pore-lining region point mutation. *Receptors Channels* **9**:353–361.

Carbone AL, Moroni M, Groot-Kormelink PJ, and Bermudez I (2009) Pentameric concatenated (alpha4)(2)(beta2)(3) and (alpha4)(3)(beta2)(2) nicotinic acetylcholine receptors: subunit arrangement determines functional expression. *Br J Pharmacol* **156**:970–981.

Celie PHN, van Rossum-Fikkert SE, van Dijk WJ, Brejc K, Smit AB, and Sixma TK (2004) Nicotine and carbamylcholine binding to nicotinic acetylcholine receptors as studied in AChBP crystal structures. *Neuron* **41**:907–914.

Chang Y, Ghansah E, Chen Y, Ye J, and Weiss DS (2002) Desensitization mechanism of GABA receptors revealed by single oocyte binding and receptor function. *J Neurosci* **22**:7982–7990.

Cooper E, Couturier S, and Ballivet M (1991) Pentameric structure and subunit stoichiometry of a neuronal nicotinic acetylcholine receptor. *Nature* **350**:235–238.

Cordero-Erausquin M, Marubio LM, Klink R, and Changeux JP (2000) Nicotinic receptor function: new perspectives from knockout mice. *Trends Pharmacol Sci* **21**: 211–217.

Corringer PJ, Le Novère N, and Changeux JP (2000) Nicotinic receptors at the amino acid level. *Annu Rev Pharmacol Toxicol* **40**:431–458.

Eaton JB, Peng JH, Schroeder KM, George AA, Fryer JD, Krishnan C, Buhlman L, Kuo YP, Steinlein O, and Lukas RJ (2003) Characterization of human alpha 4 beta 2-nicotinic acetylcholine receptors stably and heterologously expressed in native nicotinic receptor-null SH-EP1 human epithelial cells. *Mol Pharmacol* **64**: 1283–1294.

Flores CM, Rogers SW, Pabreza LA, Wolfe BB, and Kellar KJ (1992) A subtype of nicotinic cholinergic receptor in rat brain is composed of alpha 4 and beta 2 subunits and is up-regulated by chronic nicotine treatment. *Mol Pharmacol* **41**: 31–37.

Galzi JL, Bertrand D, Devillers-Thiéry A, Revah F, Bertrand S, and Changeux JP (1991) Functional significance of aromatic amino acids from three peptide loops of the α 7 neuronal nicotinic receptor site investigated by site-directed mutagenesis. *FEBS Lett* **294**:198–202.

Gentry CL, Wilkins LH, Jr, and Lukas RJ (2003) Effects of prolonged nicotinic ligand exposure on function of heterologously expressed, human alpha4beta2- and alpha4beta4-nicotinic acetylcholine receptors. *J Pharmacol Exp Ther* **304**: 206–216.

Gotti C, Clementi F, Fornari A, Gaimarri A, Guiducci S, Manfredi I, Moretti M, Pedrazzi P, Pucci L, and Zoli M (2009) Structural and functional diversity of native brain neuronal nicotinic receptors. *Biochem Pharmacol* **78**:703–711.

Gotti C, Moretti M, Meinerz NM, Clementi F, Gaimarri A, Collins AC, and Marks MJ (2008) Partial deletion of the nicotinic cholinergic receptor alpha 4 or beta 2 subunit genes changes the acetylcholine sensitivity of receptor-mediated 86Rb+ efflux in cortex and thalamus and alters relative expression of alpha 4 and beta 2 subunits. *Mol Pharmacol* **73**:1796–1807.

Grønlien JH, Håkerud M, Ween H, Thorin-Hagene K, Briggs CA, Gopalakrishnan M, and Malysz J (2007) Distinct profiles of α7 nAChR positive allosteric modulation revealed by structurally diverse chemotypes. *Mol Pharmacol* **72**:715–724.

Harpsøe K, Ahring PK, Christensen JK, Jensen ML, Peters D, and Balle T (2011) Unraveling the high- and low-sensitivity agonist responses of nicotinic acetylcholine receptors. *J Neurosci* **31**:10759–10766.

Kozikowski AP, Eaton JB, Bajjuri KM, Chellappan SK, Chen Y, Karadi S, He R, Caldarone B, Manzano M, and Yuen PW, et al. (2009) Chemistry and pharmacology of nicotinic ligands based on 6-[5-(azetidin-2-ylmethoxy)pyridin-3-yl]hex-5-yn-1-ol (AMOP-H-OH) for possible use in depression. *ChemMedChem* **4**:1279–1291.

Kuhse J, Laube B, Magalei D, and Betz H (1993) Assembly of the inhibitory glycine receptor: identification of amino acid sequence motifs governing subunit stoichiometry. *Neuron* **11**:1049–1056.

Kuryatov A and Lindstrom J (2011) Expression of functional human α6β2β3* acetylcholine receptors in Xenopus laevis oocytes achieved through subunit chimeras and concatamers. *Mol Pharmacol* **79**:126–140.

Lai A, Parameswaran N, Khwaja M, Whiteaker P, Lindstrom JM, Fan H, McIntosh JM, Grady SR, and Quik M (2005) Long-term nicotine treatment decreases striatal alpha 6* nicotinic acetylcholine receptor sites and function in mice. *Mol Pharmacol* **67**:1639–1647.

Lindstrom JM (2003) Nicotinic acetylcholine receptors of muscles and nerves: Comparison of their structures, functional roles, and vulnerability to pathology. *Ann N Y Acad Sci* **998**:41-52.

Lukas RJ and Cullen MJ (1988) An isotopic rubidium ion efflux assay for the functional characterization of nicotinic acetylcholine receptors on clonal cell lines. *Anal Biochem* **175**:212–218.

Marks MJ, Meinerz NM, Brown RWB, and Collins AC (2010) 86Rb+ efflux mediated by alpha4beta2*-nicotinic acetylcholine receptors with high and low-sensitivity to stimulation by acetylcholine display similar agonist-induced desensitization. *Biochem Pharmacol* **80**:1238–1251.

Marks MJ, Whiteaker P, Calcaterra J, Stitzel JA, Bullock AE, Grady SR, Picciotto MR, Changeux JP, and Collins AC (1999) Two pharmacologically distinct components of nicotinic receptor-mediated rubidium efflux in mouse brain require the beta2 subunit. *J Pharmacol Exp Ther* **289**:1090–1103.

Mazzaferro S, Benallegue N, Carbone A, Gasparri F, Vijayan R, Biggin PC, Moroni M, and Bermudez I (2011) Additional acetylcholine (ACh) binding site at α4/α4 interface of (α4β2)2α4 nicotinic receptor influences agonist sensitivity. *J Biol Chem* **286**:31043–31054.

Moroni M, Vijayan R, Carbone A, Zwart R, Biggin PC, and Bermudez I (2008) Non-agonist-binding subunit interfaces confer distinct functional signatures to the alternate stoichiometries of the alpha4beta2 nicotinic receptor: an alpha4-alpha4 interface is required for Zn2+ potentiation. *J Neurosci* **28**:6884–6894.

Nelson ME, Kuryatov A, Choi CH, Zhou Y, and Lindstrom J (2003) Alternate stoichiometries of alpha4beta2 nicotinic acetylcholine receptors. *Mol Pharmacol* **63**: 332–341.

Picciotto MR, Zoli M, Léna C, Bessis A, Lallemand Y, Le Novère N, Vincent P, Pich EM, Brûlet P, and Changeux JP (1995) Abnormal avoidance learning in mice lacking functional high-affinity nicotine receptor in the brain. *Nature* **374**:65–67.

Rayes D, De Rosa MJ, Sine SM, and Bouzat C (2009) Number and locations of agonist binding sites required to activate homomeric Cys-loop receptors. *J Neurosci* **29**: 6022–6032.

Seo S, Henry JT, Lewis AH, Wang N, and Levandoski MM (2009) The positive allosteric modulator morantel binds at noncanonical subunit interfaces of neuronal nicotinic acetylcholine receptors. *J Neurosci* **29**:8734–8742.

Sigel E and Buhr A (1997) The benzodiazepine binding site of GABAA receptors. *Trends Pharmacol Sci* **18**:425–429.

Steinlein OK (2001) Genes and mutations in idiopathic epilepsy. *Am J Med Genet* **106**:139–145.

Timmermann DB, Sandager-Nielsen K, Dyhring T, Smith M, Jacobsen AM, Nielsen EØ, Grunnet M, Christensen JK, Peters D, and Kohlhaas K, et al. (2012) Augmentation of cognitive function by NS9283, a stoichiometry-dependent positive allosteric modulator of α2- and α4-containing nicotinic acetylcholine receptors. *Br J Pharmacol* **167**:164–182.

Whiteaker P, Cooper JF, Salminen O, Marks MJ, McClure-Begley TD, Brown RWB, Collins AC, and Lindstrom JM (2006) Immunolabeling demonstrates the interdependence of mouse brain α4 and β2 nicotinic acetylcholine receptor subunit expression. *J Comp Neurol* **499**:1016–1038.

Whiteaker P, Wilking JA, Brown RWB, Brennan RJ, Collins AC, Lindstrom JM, and Boulter J (2009) Pharmacological and immunochemical characterization of alpha2* nicotinic acetylcholine receptors (nAChRs) in mouse brain. *Acta Pharmacol Sin* **30**:795–804.

Whiting P and Lindstrom J (1987) Purification and characterization of a nicotinic acetylcholine receptor from rat brain. *Proc Natl Acad Sci USA* **84**:595–599.

Whiting PJ and Lindstrom JM (1988) Characterization of bovine and human neuronal nicotinic acetylcholine receptors using monoclonal antibodies. *J Neurosci* **8**: 3395–3404.

Williams DK, Wang J, and Papke RL (2011) Investigation of the molecular mechanism of the α7 nicotinic acetylcholine receptor positive allosteric modulator PNU-120596 provides evidence for two distinct desensitized states. *Mol Pharmacol* **80**: 1013–1032.

Xiao YX, Fan H, Musachio JL, Wei ZL, Chellappan SK, Kozikowski AP, and Kellar KJ (2006) Sazetidine-A, a novel ligand that desensitizes alpha4beta2 nicotinic acetylcholine receptors without activating them. *Mol Pharmacol* **70**:1454–1460.

Xiu X, Puskar NL, Shanata JAP, Lester HA, and Dougherty DA (2009) Nicotine binding to brain receptors requires a strong cation-pi interaction. *Nature* **458**:534–537.

Zhou Y, Nelson ME, Kuryatov A, Choi C, Cooper J, and Lindstrom J (2003) Human alpha4beta2 acetylcholine receptors formed from linked subunits. *J Neurosci* **23**: 9004–9015.

Zwart R, Carbone AL, Moroni M, Bermudez I, Mogg AJ, Folly EA, Broad LM, Williams AC, Zhang D, and Ding C, et al. (2008) Sazetidine-A is a potent and selective agonist at native and recombinant alpha 4 beta 2 nicotinic acetylcholine receptors. *Mol Pharmacol* **73**:1838–1843.

Zwart R and Vijverberg HPM (1998) Four pharmacologically distinct subtypes of alpha4beta2 nicotinic acetylcholine receptor expressed in Xenopus laevis oocytes. *Mol Pharmacol* **54**:1124–1131.

Address correspondence to: Dr. Paul Whiteaker, Laboratory of Neurochemistry, Division of Neurobiology, Barrow Neurologic Institute, 350 West Thomas Road, Phoenix, AZ 85013. E-mail: paul.whiteaker@dignityhealth.org